DNA 4320F

VALIDATION AND REFINEMENT OF THE DELFIC CLOUD RISE MODULE

Atmospheric Science Associates
P.O. Box 307
Bedford, Massachusetts 01730

15 January 1977

Final Report for Period 28 October 1975—22 December 1975

CONTRACT No. DNA 001-76-C-0010

THIS WORK SPONSORED BY THE DEFENSE NUCLEAR AGENCY
UNDER RDT&E RMSS CODE B3250764 V99QAXNA01102 H2590D.

Prepared for
Director
DEFENSE NUCLEAR AGENCY
Washington, D. C. 20305

Destroy this report when it is no longer needed. Do not return to sender.

UNCLASSIFIED

SECURITY CLASSIFICATION OF THIS PAGE (When Data Entered)

REPORT DOCUMENTATION PAGE

READ INSTRUCTIONS BEFORE COMPLETING FORM

1. REPORT NUMBER: DNA 4320F ✓
2. GOVT ACCESSION NO.
3. RECIPIENT'S CATALOG NUMBER

4. TITLE (and Subtitle): VALIDATION AND REFINEMENT OF THE DELFIC CLOUD RISE MODULE.

5. TYPE OF REPORT & PERIOD COVERED: Final Report, for Period 28 Oct [illegible]—22 Dec 75,

6. PERFORMING ORG. REPORT NUMBER

7. AUTHOR(s): Hillyer G. Norment

8. CONTRACT OR GRANT NUMBER(s): DNA [illegible]-76-C-[illegible]

9. PERFORMING ORGANIZATION NAME AND ADDRESS: Atmospheric Science Associates ✓, P.O. Box 307, Bedford, Massachusetts 01730

10. PROGRAM ELEMENT, PROJECT, TASK AREA & WORK UNIT NUMBERS: NWED Subtask V99QAXNA011-02; A011

11. CONTROLLING OFFICE NAME AND ADDRESS: Director, Defense Nuclear Agency, Washington, D.C. 20305

12. REPORT DATE: 15 Jan[illegible] 1977

13. NUMBER OF PAGES: 60

14. MONITORING AGENCY NAME & ADDRESS (if different from Controlling Office): 57p.

15. SECURITY CLASS (of this report): UNCLASSIFIED

15a. DECLASSIFICATION/DOWNGRADING SCHEDULE

16. DISTRIBUTION STATEMENT (of this Report): Approved for public release; distribution unlimited. DNA, SBIE

17. DISTRIBUTION STATEMENT (of the abstract entered in Block 20, if different from Report)

18. 4320F, AD-E300 020

19. SUPPLEMENTARY NOTES: This work sponsored by the Defense Nuclear Agency under RDT&E RMSS Code B325076464 V99QAXNA01102 H2590D.

20. KEY WORDS (Continue on reverse side if necessary and identify by block number): Nuclear Cloud Rise; DELFIC; Fallout Prediction

21. ABSTRACT (Continue on reverse side if necessary and identify by block number): The DELFIC Cloud Rise Module is refined to produce best agreement with stabilized cloud top heights observed from 53 nuclear test shots in the yield range from 21 T to 15 MT. Agreement with observed data, for both cloud tops and bases, is shown to be excellent in the yield range from 0.5 T to 15 MT. Simulated cloud rise and growth also are shown to be in accord with observation.

DD FORM 1473 EDITION OF 1 NOV 65 IS OBSOLETE

UNCLASSIFIED

SECURITY CLASSIFICATION OF THIS PAGE (When Data Entered)

392 152

4B

20. ABSTRACT (Continued)

DELFIC cloud top height results are compared with results calculated from a power function of yield. The power function is obtained by least squares curve fitting to observed data. DELFIC yields a proportional reduction in variance of cloud top discrepancies in log space of 59 percent.

Sensitivity of results to model structure and to various parameter values is discussed.

Use of the model for very high yields (20 to 100 MT) is explored. Limitations of model capability in this yield range are pointed out, and apparent anomalous results are explained.

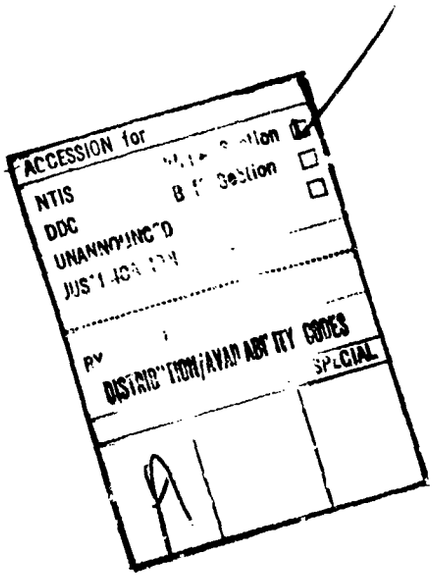

SUMMARY

The CRM differential equations are stated in simplified form, and refined values for model parameters and initial conditions are presented and discussed.

Detailed comparisons of simulation results with observed data are presented over the yield range from 0.5 T to 15 MT, with emphasis on the range 10 T to 15 MT. Comparisons are mostly for stabilized cloud dimensions, but some comparisons of temporal cloud development are included. Considering the scatter and uncertainty of observed data, the comparisons indicate excellent agreement for the most part, though there may be a tendency to overpredict base heights for very low yield shots (see Figs. 1-6).

Compared with a simple power function of yield fitted to the observed data by least squares (eq. (13)), CRM results yield a 59% reduction in the variance of $\log(z_T)_{calc} - \log(z_T)_{obs}$.

Non-linearity of the model makes it very difficult to estimate a priori the effects of changes in: model structure, parameter values, and initial conditions. Results are sensitive to changes in cloud shape, the turbulence parameter k_2, and the entrainment parameter μ. Furthermore, these interact in complex ways. One must proceed with caution in making changes, and effects of changes must be assessed via thorough study of simulation results across the complete range of yields.

Fundamental deficiencies in the model, which are especially acute at extremely high yields, are pointed out. Extrapolation of usage to the yield range 20-100MT results in apparent anomalous results, which are explained as resulting from the deficiencies. Use of the model for such high yields is questionable, especially since observations are not available for model calibration and validation.

TABLE OF CONTENTS

LIST OF FIGURES

1. INTRODUCTION

Prediction of local fallout transport and deposition is critically dependent on the height and dimensions of the stabilized nuclear cloud. Most prediction calculations begin with stabilized clouds whose dimensions are similar to those produced by test shots at the Nevada Test Site and the Marshall Islands. This provides no flexibility to account for effects of atmospheres that have different stability structures from those typical of the test locations. The DELFIC Cloud Rise Module (CRM) uses a dynamic model of cloud rise that adequately accounts for atmospheric stability, as well as for many other variables that may be significant.

The CRM is based on the water-surface-burst cloud model developed at the Naval Radiological Defense Laboratory (NRDL)[1,2]. Details of the mathematical basis of the model and of the CRM code are given by Norment and Woolf[3].

Various individuals have worked on application of the model to land-fallout prediction over the span of ten years since it was first adapted for use in DELFIC. However, the work reported here is the first really comprehensive, thorough calibration and validation study that has been done.

The CRM model is refined and its strengths and weaknesses are explored and described.

2. THE DELFIC CLOUD RISE MODULE

2.1 DESCRIPTION

The DELFIC CRM is a dynamic, one-dimensional, entraining buoble model of nuclear cloud rise. It consists of a set of coupled ordinary differential equations that represent conservation of momentum, mass, heat and turbulent kinetic energy. The nuclear cloud is defined in terms of: vertical coordinate of its center (the cloud is in some respects treated as a point)*, cloud volume, average temperature, average turbulent energy density, and the masses of its constituents: air, soil, weapon debris, water vapor and condensed water. Cloud properties and contents are taken to be uniform over the cloud volume.

Initial conditions are specified at approximately the time the fireball reaches pressure equilibrium with the atmosphere. Atmospheric conditions (vertical profiles of pressure, temperature and relative humidity) are accepted by the CRM in tabular form.

Effects of initial conditions and atmospheric stability on the cloud rise are accounted for because of the dynamic nature of the model. Atmospheric stability is especially important in determining the stabilized height of the cloud, which, in turn, is critical in determining the distribution of local fallout on the ground.

The differential equations are solved by a fourth-order Runge-Kutta algorithm. Complete simulations are very fast on a modern computer.

Equations, parameters and initial conditions presented in this chapter are for the refined version of the CRM, which has evolved, in part, from the studies discussed herein.

---

* Effects of this model limitation on rise simulation of very large clouds are discussed in Chapter 4.

2.2 SIMPLIFIED EQUATIONS

The CRM conservation equations are those developed by Huebsch for a water-surface burst[1,2] as modified by Norment and Woolf (ref. 3, Appendix C.1). The simplified equations given here are for a pure-air cloud in a dry atmosphere. The more complex equations that account for the presence of water and soil are given in ref. 3. For all CRM calculations, including those described here, the complete equations are used. Effects of water and soil are deleted solely for this presentation to reduce algebraic complexity. To further increase understanding, each equation term is identified as to function. (Symbols are defined in Appendix A below.)

2.2.1 Momentum

$$\frac{du}{dt} = \overset{(a)}{\left(\frac{T}{T_e} - 1\right) g} - \left[\overset{(b)}{\frac{2k_2 v}{H_c} \frac{T}{T_e}} + \overset{(c)}{\frac{1}{m} \frac{dm}{dt}} \right] u \qquad (1)$$

Terms (a), (b) and (c) represent forces due to buoyancy, eddy-viscous drag and entrainment drag respectively. This is the only equation that differs from the most recent predecessor model described in ref. 3. The asymmetric entrainment factor $(1 - \mu)$ and the factor containing the virtual mass $\left(\frac{m}{m+m_i}\right)$ have been dropped. Deletion of these factors causes negligible change in prediction results.

2.2.2 Center Height.

$$\frac{dz}{dt} = u \qquad (2)$$

2.2.3 Temperature

$$\frac{dT}{dt} = -\frac{1}{c_p} \left[\overset{(a)}{\frac{T}{T_e} gu} + \overset{(b)}{c_p (T - T_e)} \overset{(c)}{\frac{1}{m} \frac{dm}{dt}} - \varepsilon \right] \qquad (3)$$

Terms (a), (b) and (c) account for the effects of adaibatic expansion, entrainment and dissipation of turbulent energy to heat (see eq. (4a)) respectively.

2.2.4 Turbulent Kinetic Energy Density

$$\frac{dE}{dt} = \underbrace{2k_2 \frac{T}{T_e} \frac{u^2 v}{H_c}}_{(a)} + \underbrace{\frac{u^2}{2} \frac{1}{m} \frac{dm}{dt}}_{(b)} - \underbrace{E \frac{1}{m} \frac{dm}{dt}}_{(c)} - \underbrace{\varepsilon}_{(d)} \tag{4}$$

Terms (a) and (b) account for turbulent energy generated by the mean flow via eddy-viscous drag and momentum-conserving inelastic-collision entrainment respectively. Term (c) represents entrainment dilution, and (d) represents dissipation to heat, where the turbulent dissipation rate, ε, is

$$\varepsilon = \frac{k_3 (2E)^{3/2}}{H_c} \tag{4a}$$

2.2.5 Mass

$$\frac{dm}{dt} = m \frac{T}{T_e} \left[\underbrace{\frac{S}{V} \mu v}_{(a)} + \underbrace{\frac{1}{c_p T} \left(\frac{T}{T_e} gu - \varepsilon \right)}_{(b)\ (c)} - \underbrace{\frac{gu}{R_a T_e}}_{(d)} \right] \tag{5}$$

This equation is based on observed volumetric growth of nuclear clouds, and term (a) contains this information. The other terms are required to convert volumetric to mass growth rate. Terms (b) and (c) account for temperature effects caused by entrainment and conversion of turbulence energy to heat, and term (d) accounts for hydrostatic expansion of the rising cloud.

2.3 DIMENSIONLESS PARAMETERS

Three empirical, dimensionless parameters are of interest here. All are held constant during a cloud rise simulation.

2.3.1 Energy Conversion Parameter, k_2.

The terms in eqs. (1) and (4) that contain k_2 represent conversion of kinetic energy of rise to turbulent kinetic energy. Since I have no way to judge a priori what the value of k_2 should be, I have taken it to be an adjustable parameter. Good prediction results are obtained with

$$k_2 = \max \left[\; 0.004, \min(0.1, \; 0.1W^{-1/3}) \; \right] \tag{6}$$

In long form, this equation means:

$$k_2 = 0.1 \quad , \qquad W < 1 \text{ kT}$$

$$k_2 = 0.1W^{-1/3} \quad , \qquad 1 \leq W \leq 15{,}625 \text{ kT}$$

$$k_2 = 0.004 \quad , \qquad 15{,}625 < W \quad \text{kT}$$

Restriction to a maximum value of 0.1 at low yields was found to be necessary to prevent underprediction for low yield shots. Restriction to a minimum value of 0.004 at very high yields is discussed in sec. 4.2.

2.3.2 Turbulent Energy Dissipation Parameter, k_3.

k_3 appears in eq. (4a). It is given the constant value 0.175, which is unchanged from the original NRDL version of the model[2].

2.3.3 Entrainment Parameter, μ.

The entrainment parameter appears in eq. (5). As explained in Appendix C.1 of ref. 3, it is related to the altitude gradient of linear cloud dimension during the early portion of nuclear cloud rise. In the preceding CRM version, we computed μ as a function of yield from an equation

$$\mu = 0.092W^{0.13}$$

that was obtained by Norment and Woolf[4] from the vertical gradients of horizontal radii for a set of observed cloud rise data. Since this data set was not very large, and since one cannot be sure that horizontal radius is the proper cloud dimension to use, I have simplified this relation slightly. Good prediction results are given by

$$\mu = \max\left[\max(0.12,\ 0.1W^{0.1}) \ ,\ 0.01W^{1/3} \right] \qquad (7)$$

In long form this equation means:

$$\mu = 0.12 \quad , \quad W \leq 6.192 \text{ kT}$$

$$\mu = 0.1W^{0.1} \quad , \quad 6.192 \leq W \leq 19{,}307 \text{ kT}$$

$$\mu = 0.01W^{1/3} \quad , \quad 19{,}307 \leq W \text{ kT}$$

it was found necessary to use a constant value of $\mu = 0.12$ for low yield shots because of a tendency to overpredict for low yields.* The change from 1/10 to 1/3 yield dependence at very high yields is discussed in sec. 4.2.

2.4 INITIAL CONDITIONS

Initial time (relative to detonation), initial gas phase temperature and soil loading of the cloud are the same as in the original DELFIC[5]. Only initial conditions that have been changed are discussed here.

2.4.1 Explosion Energy Fraction in the Cloud, f.

The original NRDL water-surface burst model used an energy fraction of 33%. For the first DELFIC simulations, we increased this to 50%. As a result of extensive simulations with an early version of DELFIC, we have used $f = 0.44W^{0.014}$ (W in kT), which is such a weak function of yield as to be essentially constant.

In this latest version, I simply take $f = 0.45$ for all yields.

2.4.2 Temperature of Condensed-Phase Matter.

For a surface or near surface burst, a substantial amount of soil which does not reach thermal equilibrium with the fireball gases remains in the solid or liquid state. The average temperature of this material at our initial time is

---

* If the yield dependent functions for k_2 and μ are allowed to extend into the low yield range, the tendencies for under prediction because of high k_2 and overprediction because of low μ substantially compensate. However, scatter is significantly greater for both tops and bases as is apparent from comparison of observed vs. calculated graphs and also from the agreement statistics.

conjectural but important since the energy required to heat it must be taken from that available. For very low yield shots, the soil temperature specified by the original DELFIC Initial Conditions Module (Subroutine TEMP) has been found to be too high[6].

I recommend the following initial soil temperature for future use:

$$T_{s,i} = 200 \log_{10}(W) + 1000 \quad , \tag{8}$$

where W is in kT, and $T_{s,i}$ in degrees Kelvin.

2.4.3 Altitude.

In the preceding CRM version, we used an empirical equation to determine cloud center height relative to burst point at our initial time (eq. (1.20) of ref. 3). I have simplified that expression slightly so that it is a function of $W^{1/3}$. Good results are obtained with

$$z_i = z_{GZ} + z_{HoB} + 90W^{1/3} \quad . \tag{9}$$

2.4.4 Rise Velocity.

Since 1971 my version of the CRM has used

$$u_i = 1.2\sqrt{gR_{c,i}} \quad . \tag{10}$$

The form of this equation results from a simple, approximate analysis of initial fireball rise, and the constant 1.2 is chosen to fit observed data.

2.4.5 Mass and Volume.

The energy in the cloud (45% of explosion energy) is used to heat soil and air to their respective initial temperatures. The soil mass and both initial temperatures are specified by the code[5]. The mass of air is computed via a simple energy balance as described in ref. 3. Cloud volume is taken to be equal to the volume of this mass of air.

2.5 CLOUD SHAPE

Observations of nuclear clouds show that vertical cloud dimension is a simple linear function of height during cloud rise[4]. This holds over essentially the complete rise history of nuclear clouds of all yields for which we have data. In the preceding CRM version, cloud volume was computed dynamically, and vertical cloud radius was computed as a linear function of altitude. The slope of the linear function was taken to be μ, and the intercept was computed for an ellipsoidal cloud of eccentricity 0.75 at the initial time.

Though the extensive simulations described in the next chapter have shown that the above procedure works satisfactorily, I have deleted it from this version of the CRM. This was done to avoid the possibility that this rather restrictive dependence on height and the entrainment parameter μ might occasionally produce unrealistic results.

In the new CRM, the cloud is held to the ellipsoidal shape, eccentricity 0.75, until it stops rising, after which its vertical dimension remains fixed while volume increase is accommodated by lateral expansion. The eccentricity value 0.75 is an average, with standard deviation 0.08, found by Norment and Woolf for ten test shots that cover a yield range from 3.6 kT to 15 MT[4].

Norment and Woolf found little variation of eccentricity with height, particularly for small and medium yield shots, up to the altitude at which stabilization and final horizontal expansion begins.

For a cloud with eccentricity 0.75, $H_c/R_c = 0.66144$.

2.6 TERMINATION OF RISE AND EXPANSION

Termination switches in the CRM code are discussed on pp. 48-51 of ref. 3. A normal termination was via the R-RATE switch, which operates when the relation

$$\frac{|\Delta R_c|}{\Delta t} \leq \frac{R_c W^{0.014778}}{1153} \tag{11}$$

is satisfied, where W is in kT and Δt in seconds. This switch produces reasonable results for many cases. However, it frequently causes trouble, particularly for shots at the extremities of the yield range.

For low yields, the shut-off frequently is later than desired which results in clouds that are too broad.

At the other extreme, growth rates of multi-megaton clouds tend to oscillate slowly, and if a radial expansion rate trough happens to dip below the limit given by eq. (11), shut-off occurs prematurely.

To correct the high yield problem I have added to eq. (11) the requirement that the cloud rise velocity must be zero.

For low yield shots I have added a new switch, the U,EK switch. This terminates cloud growth when the turbulent kinetic energy density falls below a threshold. Termination occurs when the following relations are satisfied

$$E < \max\left[10, \min(23 + 9 \log_{10} W, 60)\right] \tag{12}$$

and

$$u = 0 \quad .$$

In long form, these equations mean that termination occurs when

$$E < 10 \quad , \quad W \leq 0.0359 \text{ kT}$$

$$E < 23 + 9 \log_{10} W \quad , \quad 0.0359 \leq W \leq 12{,}915 \text{ kT}$$

$$E < 60 \quad , \quad 12{,}915 \leq W \text{ kT}$$

and

$$u = 0 \quad .$$

Here E is in units of Joules/kg (i.e., m^2/sec^2). It turns out that most low and medium yield cases are terminated by this switch, but megaton yield cases are terminated by the R-RATE switch.

3. COMPARISON OF PREDICTED WITH OBSERVED DATA

3.1 THE OBSERVED DATA SET

Almost all of the shots that I have considered in this study are listed in Table A.2.1 of ref. 3 (pp. 160-164). For each shot the data consist of: yield, ground zero height, height of burst, observed (at or near shot time) altitude profiles of pressure, temperature and relative humidity, observed height of the stabilized cloud top and, in most cases, observed height of the stabilized cloud base.

There are 60 shots in the set. Yields range from 0.5 ton to 15 megatons. In recalibrating and validating the model I have used the 53 shots with yields greater than 0.01 kT. Observed heights of stabilized cloud bases are available for 48 of these.

Top and base heights of the observed stabilized clouds are plotted against yield in Fig. 1. The solid lines are least squares curve fits to the data, which are given by

$$z_T = 3914W^{0.270} \tag{13}$$

and

$$z_B = 1971W^{0.307} \tag{14}$$

where z_T and z_B are in meters relative to burst height and W is in kilotons*.

The CRM code was modified such that it could batch process the complete set of data, print individual results, print stabilized height agreement statistics and plot calculated vs. observed stabilized cloud heights. Over 60 runs were made as I progressed through various sensitivity studies, modifications and

---

* These equations compare well with their counterparts, eqs. (2.1) - (2.6) in DASA-1251[7], in the yield range 0.1 to 100 kT (see Table 1).

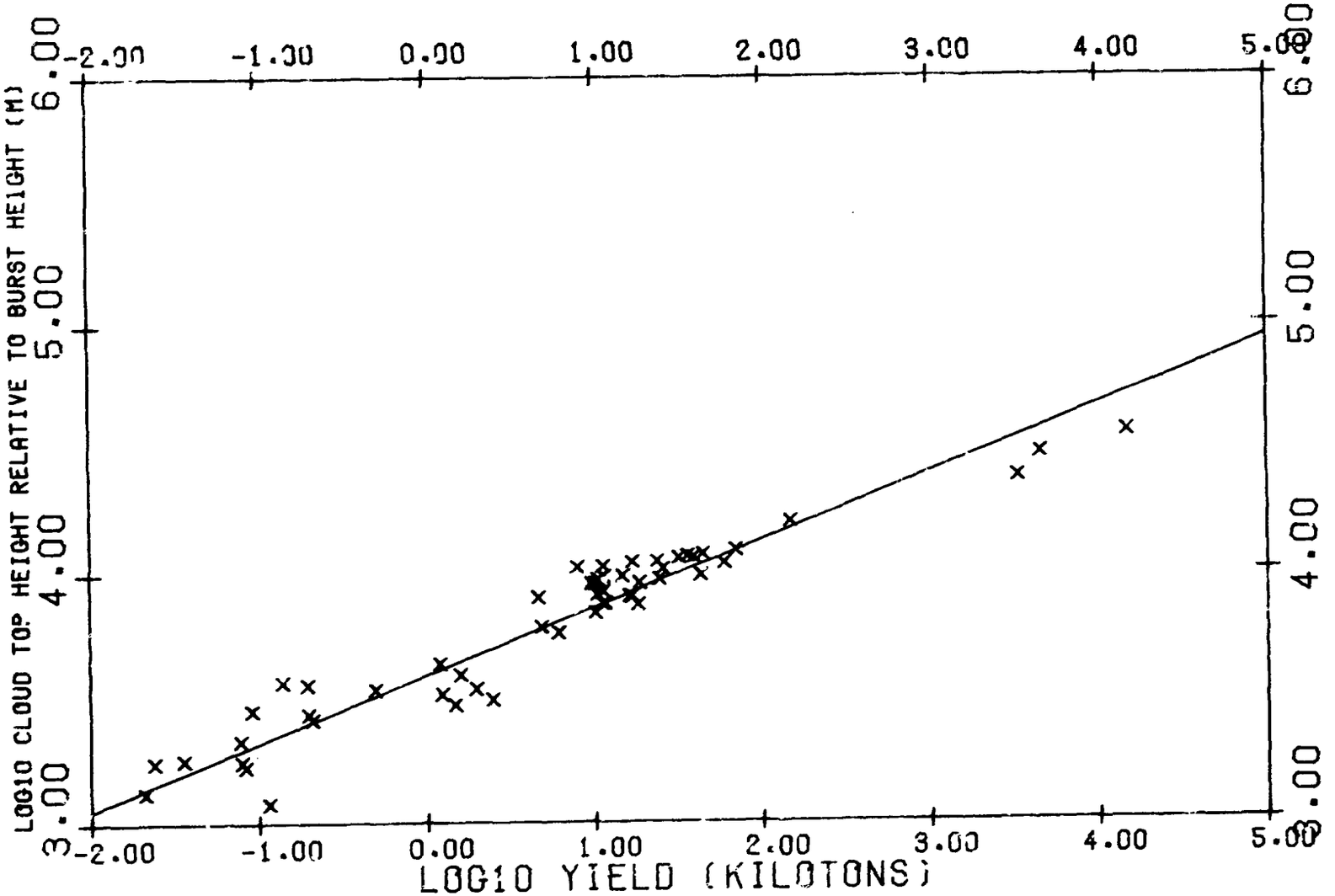

Figure 1a. Observed stabilized cloud top heights vs. yield for 53 shots in the yield range 0.021-15,000 kT. The straight line is a least squares fit to the data (see eq.(13)).

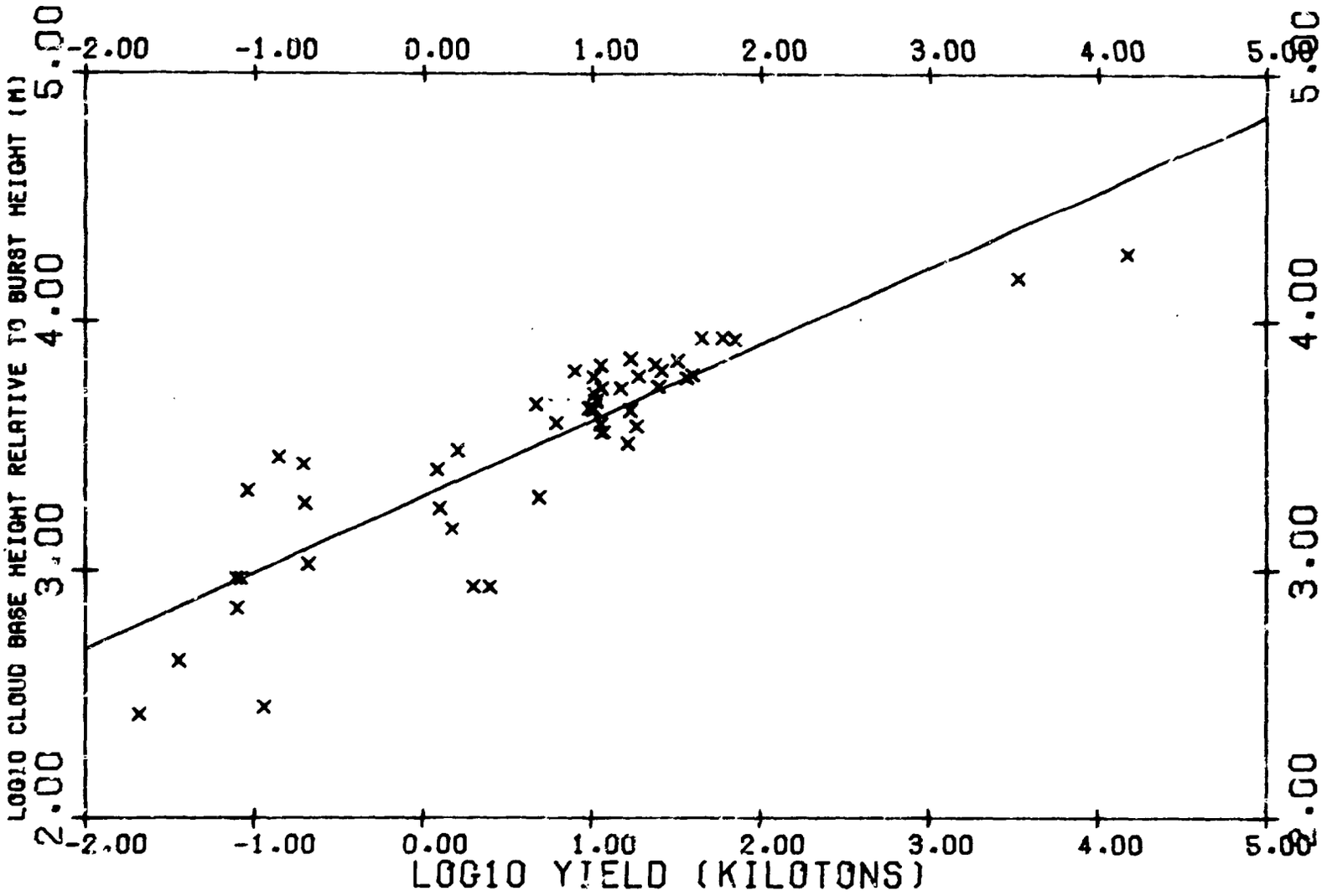

Figure 1b. Observed stabilized cloud base heights vs. yield for 48 shots in the yield range 0.021-15,000kT. The straight line is a least squares fit to the data (see eq. (14)).

refinements to the model. The complete model, including effects of water and soil, was used in all calculations.

3.2 COMPARISON CRITERIA

By far the most useful criterion for judging prediction adequacy is comparison of calculated with observed stabilized cloud top heights. This is true for the following reasons:

- Stabilized top height is the most critical cloud property in determining which winds are involved in the transport and deposition of fallout.

- Stabilized top height is by far the most accurately observed cloud property. Other stabilized cloud properties, such as base height and radius, are so poorly defined as to be virtually useless in assessing simulation accuracy.

Therefore I have relied mainly on comparison of stabilized cloud top heights in this study.

Of course, other cloud properties are of consequence and they are considered. For DELFIC predictions the least important is the height of the base of the stabilized cloud*, since fallout particle cloud bases are defined by the altitudes to which the particles have settled at stabilization time. As regards the stabilized cloud radius, it can be important in determining the crosswind spread of the fallout pattern; however, assessment of the cloud radius prediction accuracy is best made by comparing calculated with observed fallout patterns, which is not considered here. Temporal development of nuclear clouds also is of importance. CRM capability to simulate all of these cloud properties is analysed in the next section.

---

* This corresponds to the base of the visually observed cloud cap, which is also the quantity plotted in the b parts of the figures herein.

3.3 RESULTS FOR THE REFINED MODEL

3.3.1 Graphical Comparisons of Stabilized Cloud Height.

Calculated vs. observed cloud top and base heights in the yield range 0.01 - 15,000 kT are shown in Fig. 2. The tops comparison is very good over the entire yield range. For the bases there is considerable overprediction for low yields, whereas the comparison is good for medium and high yields. In light of the scatter of observed data in Fig. 1, these results can be considered to be excellent, even for the low yield bases.

Calculated vs. observed heights for all 60 cases (extending the yield range to 0.5 T) are shown in Fig. 3. Obviously the model works well at very low yields also.

3.3.2 Stabilized Cloud Height Comparison Statistics.

Agreement statistics used in the refinement are the fractional RMS deviation

$$FRMS = \sqrt{\frac{\sum^{N}\left(\frac{z_{obs}-z_{calc}}{z_{obs}}\right)^2}{N}} \qquad (15)$$

and the fractional mean deviation

$$FMD = \frac{\sum^{N}\left(\frac{z_{obs}-z_{calc}}{z_{obs}}\right)}{N} \qquad (16)$$

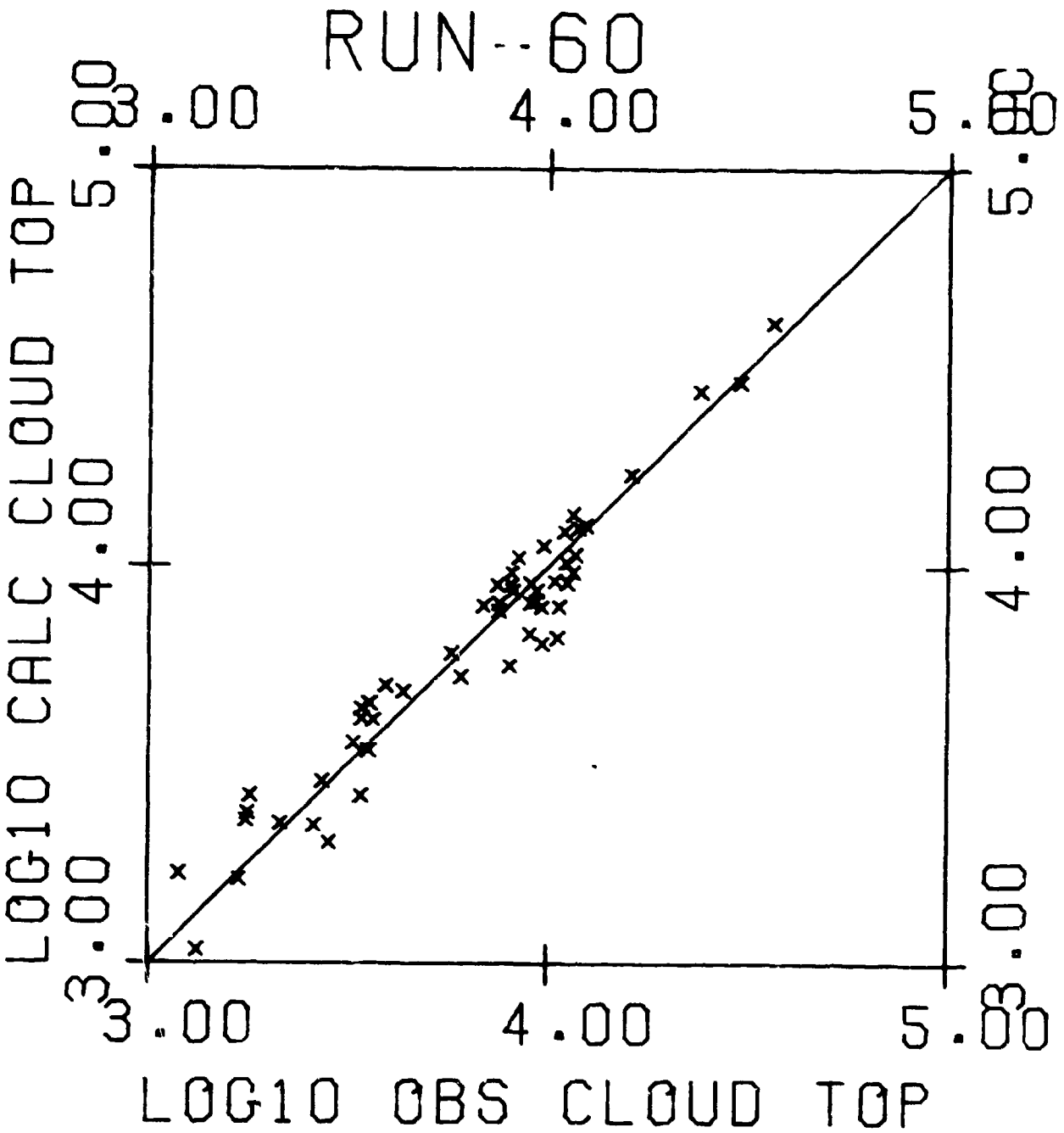

Figure 2a. Calculated vs. observed stabilized cloud top heights (meters relative to burst height) for 53 shots in the yield range 0.021-15,000 kT for the refined CRM.

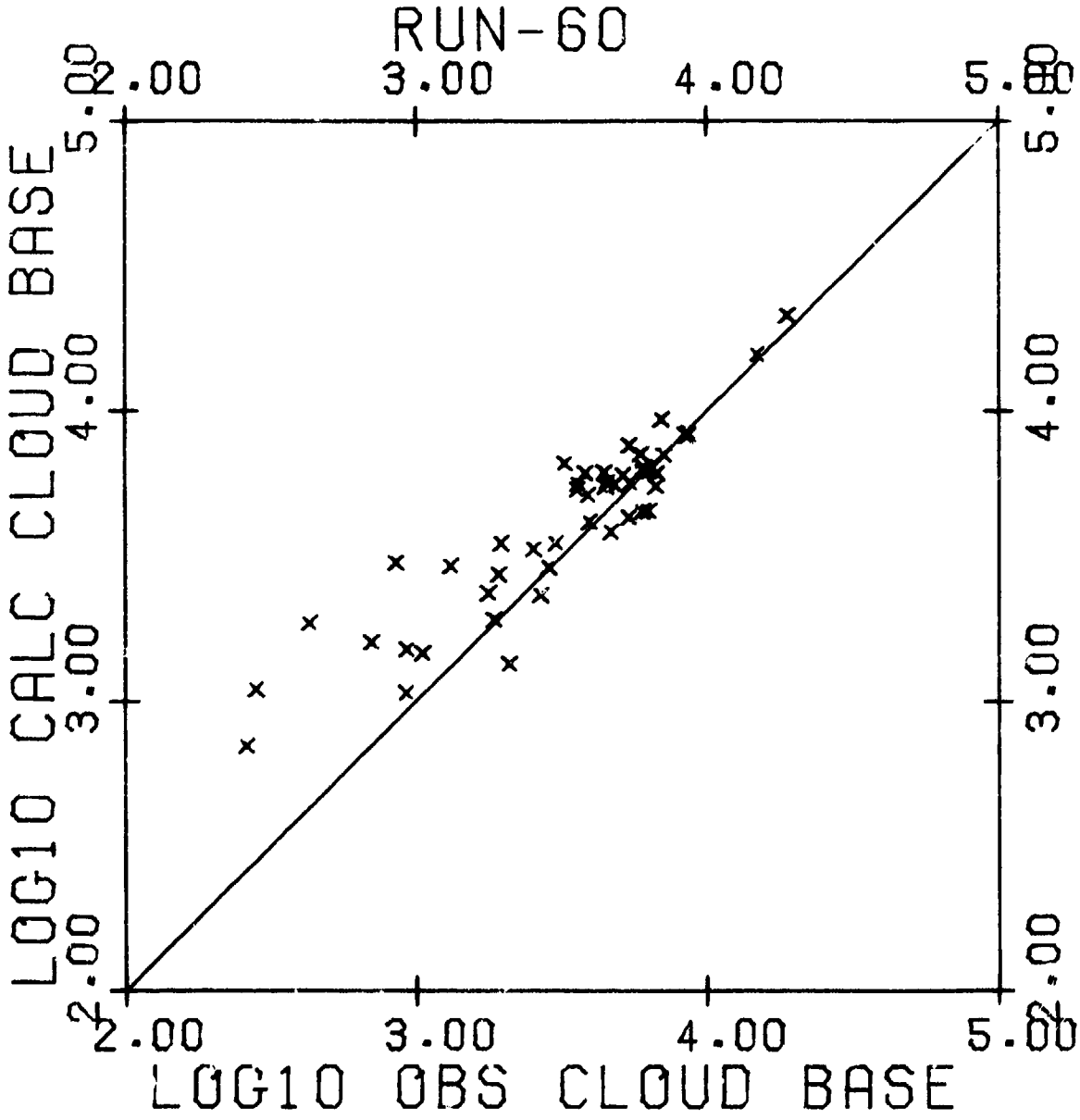

Figure 2b. Calculated vs. observed stabilized cloud base heights (meters relative to burst height) for 53 shots in the yield range 0.021-15,000 kT for the refined CRM.

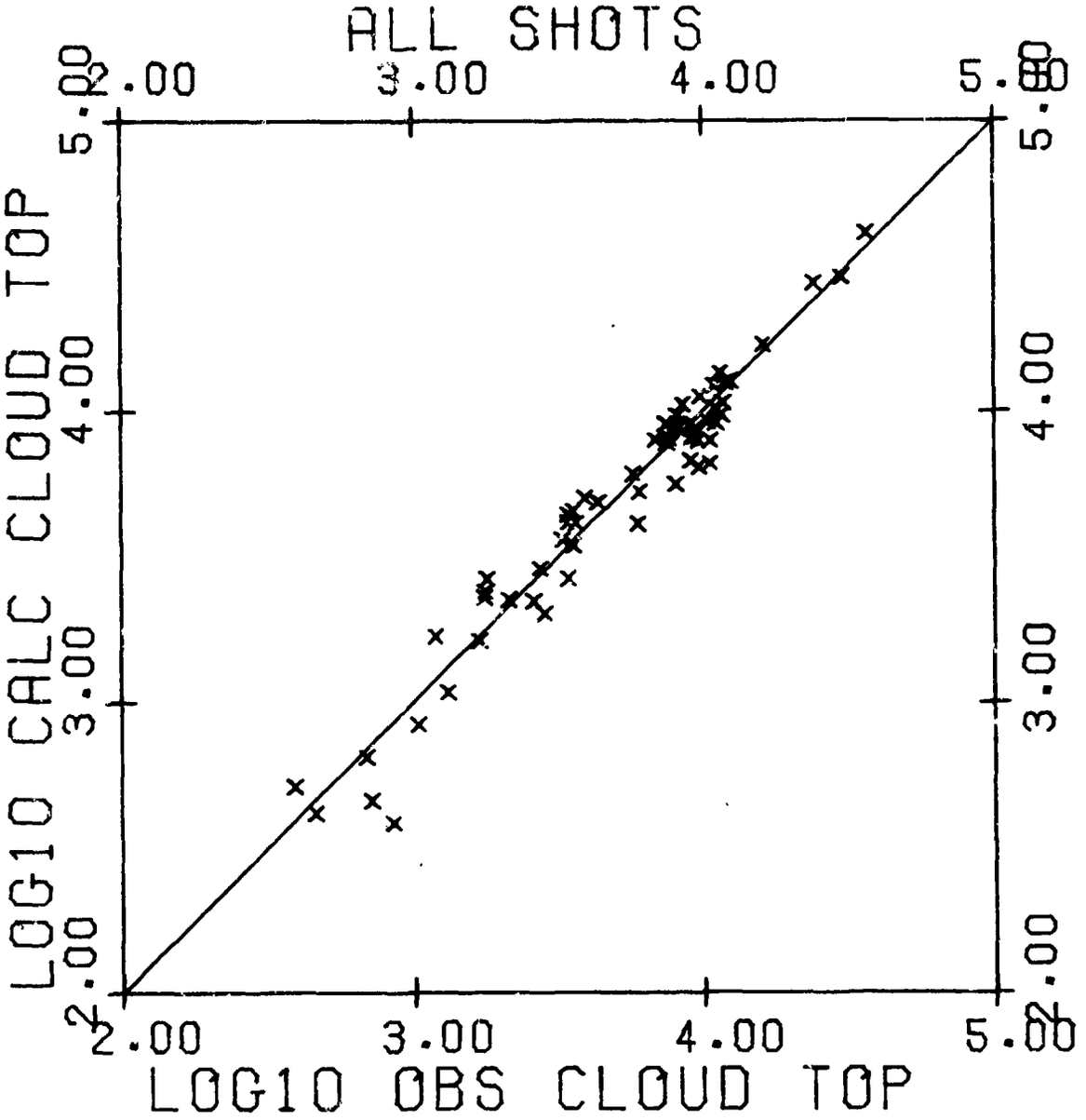

Figure 3a. Calculated vs. observed stabilized cloud top heights (meters relative to burst height) for 60 shots in the yield range 0.0005-15,000 kT for the refined CRM.

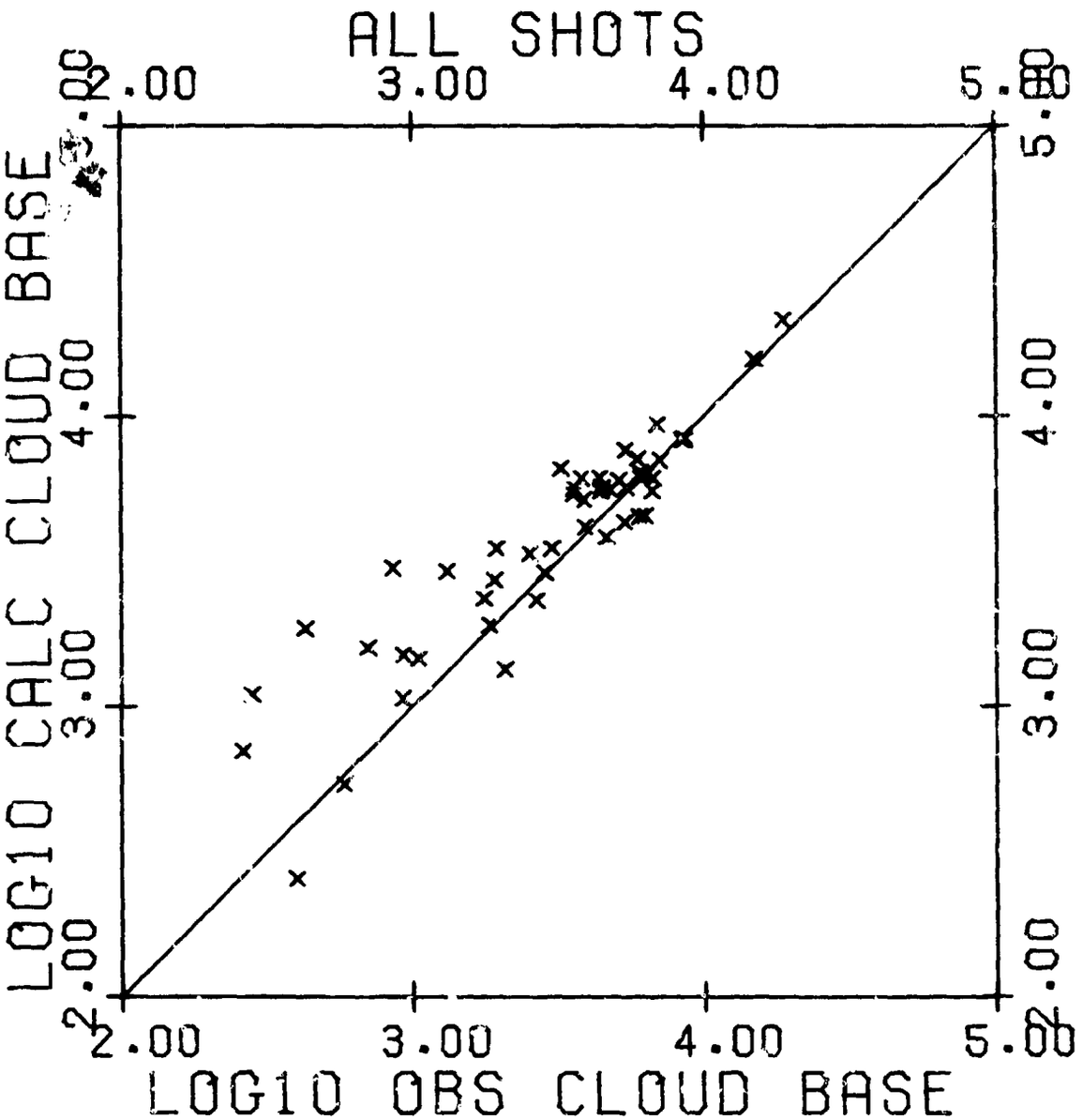

Figure 3b. Calculated vs. observed stabilized cloud base heights (meters relative to burst height) for 50 shots in the yield range 0.0012-15,000 kT for the refined CRM.

For the refined model, we have

	SHOTS FOR WHICH W > 0.01 kT		COMPLETE SET OF SHOTS	
	TOPS	BASES	TOPS	BASES
FRMS	0.15	0.29	0.14	0.29
FMD	-0.009	-0.16	0.002	-0.15

Figure 1 and eqs. (13) and (14) imply that much of the scatter of the observed data can be accounted for by expressing z_T and z_B as simple power functions of yield. For example, the least squares (LS) analysis by which eq. (13) was determined minimized the variance

$$(\sigma_T^2)_{LS} = \frac{\sum^N \left[\log_{10}(z_T)_{obs} - \log_{10}(z_T)_{LS}\right]^2}{N} \quad (17)$$

where $(z_T)_{LS}$ is the value of z_T calculated by eq. (13). An important criterion of the value of the CRM is to compare the scatter of observed data around the least squares curve with the scatter of observed data around the CRM calculated results Thus the result of eq. (17) is to be compared with

$$(\sigma_T^2)_{CRM} = \frac{\sum^N \left[\log_{10}(z_T)_{obs} - \log_{10}(z_T)_{CRM}\right]^2}{N} \quad (18)$$

where $(z_T)_{CRM}$ is the value of z_T calculated by the CRM.

Results of this comparison are:

	$(\sigma^2)_{LS}$	$(\sigma^2)_{CRM}$	N
TOPS	0.0180	0.00739	53
BASES	0.0412	0.0436	48

For the tops, the CRM affords a proportional reduction in variance of 59% relative to the simple power function of yield (eq. (13)). The ratio of variances $((\sigma_T^2)_{LS}/(\sigma_T^2)_{CRM} = 2.43)$ can be used to test whether or not the reduction in variance is significant. Using the F distribution test[8], the reduction is significant at less than the 2% level. (That is, the probability is greater than 98% that the reduction in variance is significant.) For the cloud bases, on the other hand, the power function of yield is essentially equal to the CRM as a predictor. However, as noted above, cloud base heights are very poorly defined observationally and are not critical for DELFIC fallout predictions.

It is important to realize that this success of the CRM is by no means its only virtue. Of more importance is its capability to make cloud rise predictions under atmospheric conditions that are significantly different from those encountered at the Nevada and Pacific Test Sites. For example, tropopause heights in arctic atmospheres or in northern Europe during winter are much lower than encountered at the test sites; while this would have profound effects on local distribution of fallout, it would not be accounted for by use of the empirical power function equation for cloud height.

3.3.3 Cloud Development Comparisons.

There are not many observed cloud rise histories available that are detailed enough or extend to early enough times to be of value here. Moreover, much of what is available does not correspond with our data set. Figures 4 and 5 show two comparisons available from the data on hand.* Atmospheric data observed

---

* It is instructive to note that the observed stabilized cloud heights shown in the figures do not correspond closely with the values used in our comparisons studies. For example, the observed U/K Simon top height in Fig. 5 is 16 km, whereas the value used in our comparisons is 13.3 km, while that given in ENW[9] is 13.7 km. This illustrates the considerable variation of data that is usually found in different sources.

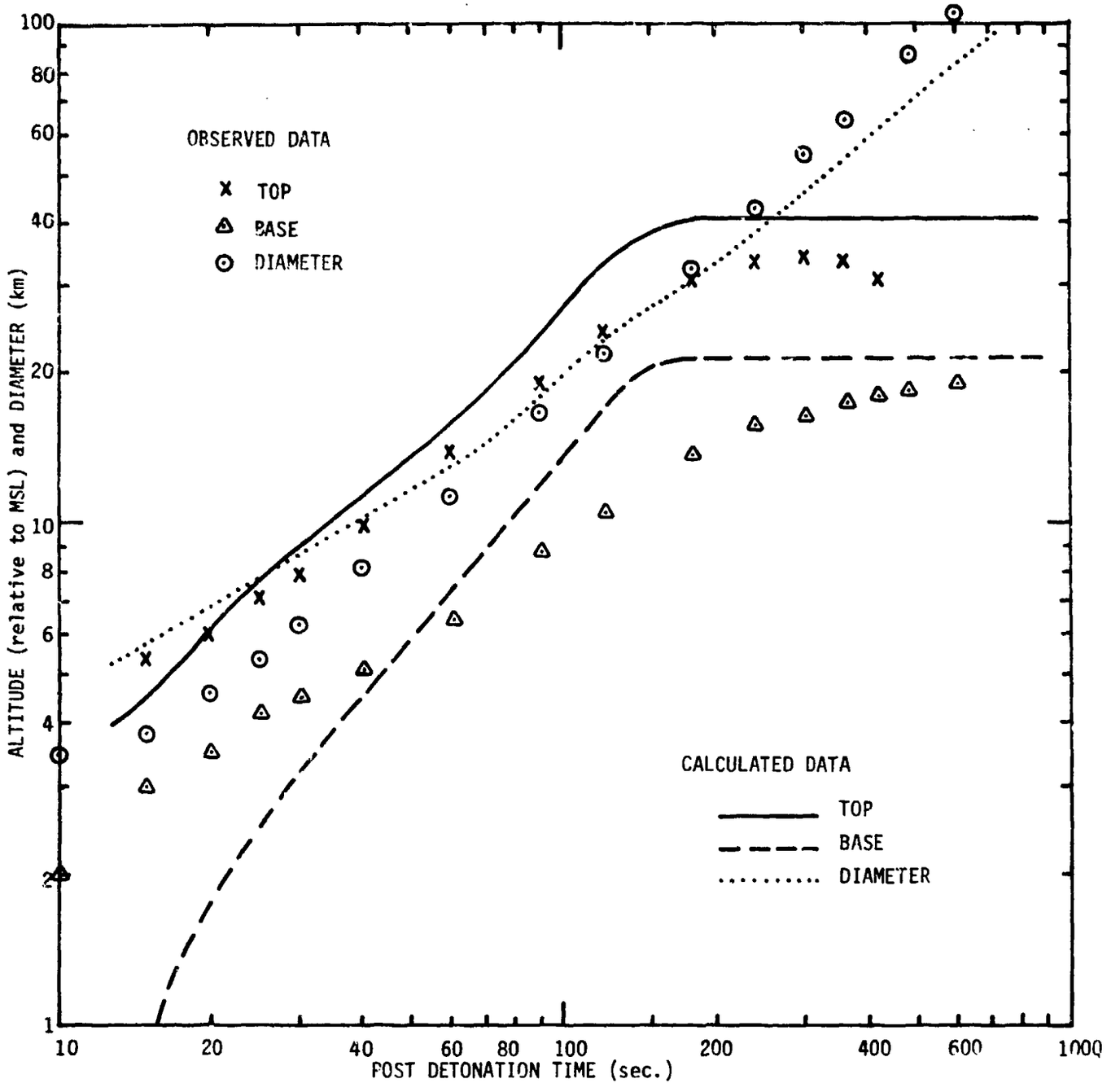

Figure 4. Observed and calculated development of the Castle Bravo cloud. Bravo was a 15 MT surface burst on Bikini Island in the Marshalls group[9]. Atmospheric data observed on-site at shot time were used in the simulation.

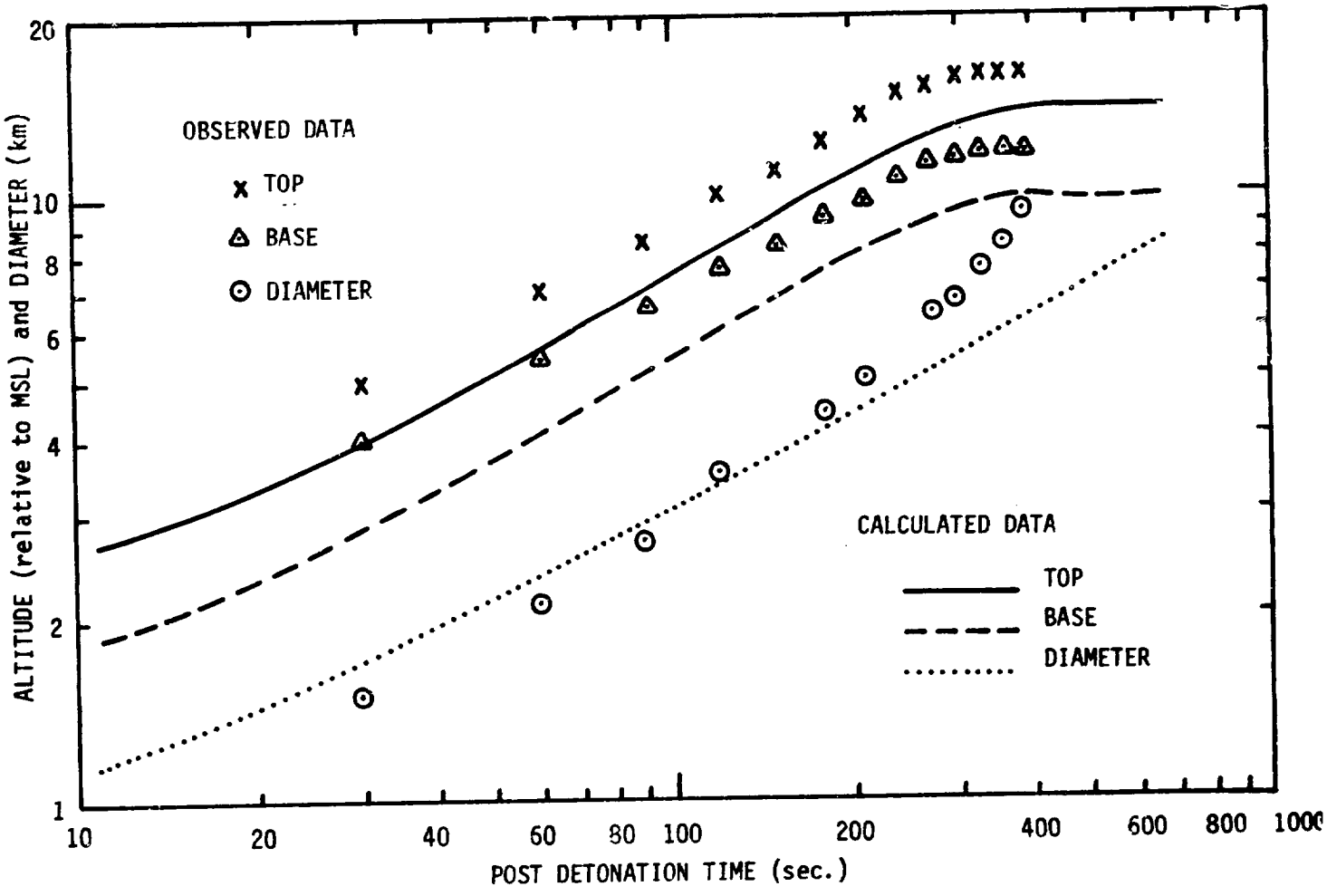

Figure 5. Observed and calculated development of the Upshot-Knothole Simon cloud. Simon was a 45 kT tower shot at the Nevada Test Site[9]. Atmospheric data observed on-site at shot time were used in the simulation. (see Footnote p.29)

near shot time are used in the simulations. Figure 6 shows calculated data for a 1.2 kT surface shot with a ground-zero height of 1284 meters. A standard atmosphere for 30°N, January was used. Observed stabilized cloud heights for Jangle-S are given for comparison.

3.3.4 Comparisons of Stabilized Cloud Dimensions with Standard Equations.

Table 1 lists stabilized cloud data for sea-level surface bursts in the mid-latitude, spring/fall standard atmosphere. Comparisons with results calculated by eqs. (13) and (14) above, and by similar equations in DASA-1251[7] are given, including cloud radii comparisons. Not surprisingly, agreement of CRM cloud top results with eq. (13), up to about 100 kT, is usually superior to agreement with the DASA-1251 equations. On the other hand, for higher yields the reverse is true. This latter is probably a reflection of the use by DASA-1251 of a separate equation for high yield shots which has a lower slope in log-log space than their curve for low yield shots.

For low yield shots, the CRM cloud base results agree better with the DASA-1251 equations than with eq. (14). This indicates that the apparent tendency for the CRM to overpredict cloud base heights, and produce a cloud that is too thin, may be more of an anomaly of the data set used here than a real problem.

The radii comparisons in Table 1 are satisfactory considering the element of subjectivity that is inevitable in defining stabilization time both in the field and in simulations.

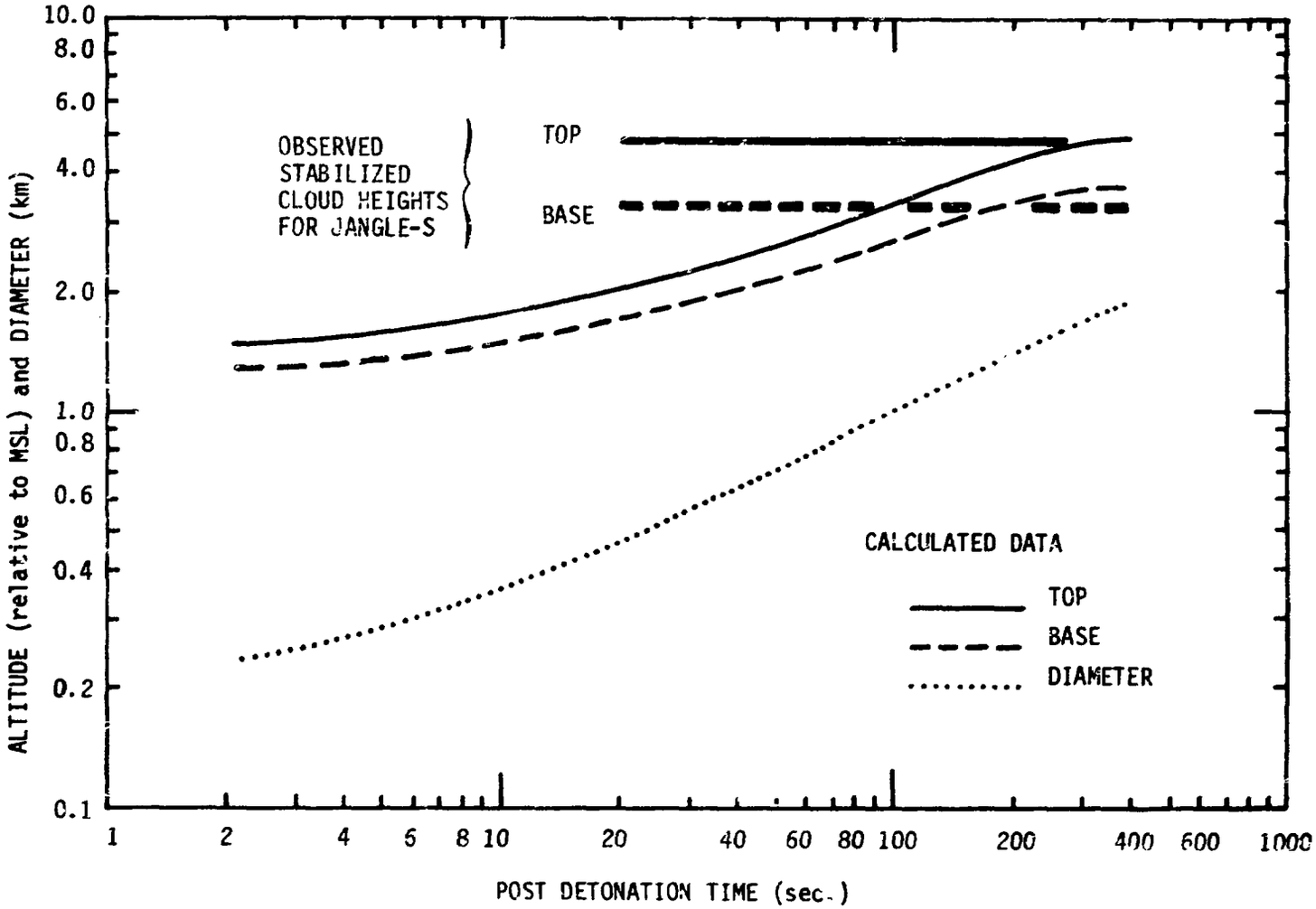

Figure 6. Calculated cloud development for a 1.2 kT surface burst at a ground zero altitude of 1284 meters. The 30°N January standard atmosphere was used in the simulation. Observed stabilized cloud heights for shot Buster-Jangle Sugar are shown[9]. (This shot is not included in our set of 60 observed cases because of the lack of observed atmospheric data.)

TABLE 1

COMPARISON OF CRM RESULTS WITH DASA-1251 EQUATIONS

YIELD (kT)	SOURCE*	STABILIZED CLOUD DIMENSIONS (meters) TOP HEIGHT	BASE HEIGHT	RADIUS
10^{-2}	CRM	1010	677	265
	Eqs.(13)&(14)	1130	479	
	DASA-1251	1301	722	122
10^{-1}	CRM	1865	1203	460
	Eqs.(13)&(14)	2103	972	
	DASA-1251	2204	1198	327
10^{0}	CRM	3210	2121	844
	Eqs.(13)&(14)	3914	1971	
	DASA-1251	3734	1987	873
10^{1}	CRM	6811	4676	1747
	Eqs.(13)&(14)	7283	3998	
	DASA-1251	6326	3290	2334
10^{2}	CRM	12194	7911	4851
	Eqs.(13)&(14)	13551	8107	
	DASA-1251	14393	9168	6239
10^{3}	CRM	18252	10748	14403
	Eqs.(13)&(14)	25217	16440	
	DASA-1251	21634	13277	16677
10^{4}	CRM	32516	16733	39478
	Eqs.(13)&(14)	46923	33339	
	DASA-1251	32519	19152	44577
10^{5}	CRM	59958	17712	178110
	Eqs.(13)&(14)	87315	67608	
	DASA-1251	48881	27499	119153

---

* CRM results are for sea-level surface bursts using the U.S. Standard Atmosphere, Mid-Latitude, Spring/Fall. DASA-1251 height results are computed from eqs.(2.1)-(2.6) of ref. 7, and the radii are computed from eq.(2.13) of ref. 7 for a stabilization time of ten minutes.

3.3.5 Comparisons Assessment.

It is clear that the DELFIC CRM adequately simulates the general features of nuclear cloud rise. Moreover, where observed data exist to provide a basis for calibration of the model, good agreement with observation is obtained.

3.4 SENSITIVITY OF RESULTS TO MODEL STRUCTURE

The CRM model consists of twelve coupled differential equations (eqs. (1) - (5) plus equations to account for water and soil content of the cloud), with large sets of initial conditions and empirical model parameters. The model is so nonlinear as to often preclude a priori estimation of the effects of changes in model structure or inputs, unless the estimates are based on extensive experience with the model. In this section I present some additional comparisons results and discuss the sensitivity of the model to its more critical or controversial structural aspects. Sensitivity to initial conditions and atmospheric structure is discussed elsewhere[10].

3.4.1 DELFIC CRM circa 1970 and 1971: Sensitivity to u_i.

Figure 7 shows calculated vs. observed stabilized cloud tops and bases for the version of the CRM described in ref. 3. The major fault with these results is unexceptional overprediction of base heights for low yield shots. Otherwise, the results are fairly good except for a tendency to underpredict top heights in the midyield-cluster of data.

In 1971 the initial rise velocity was changed from the power function of yield (eqs. 1.27 and 1.28 of ref. 3) to that

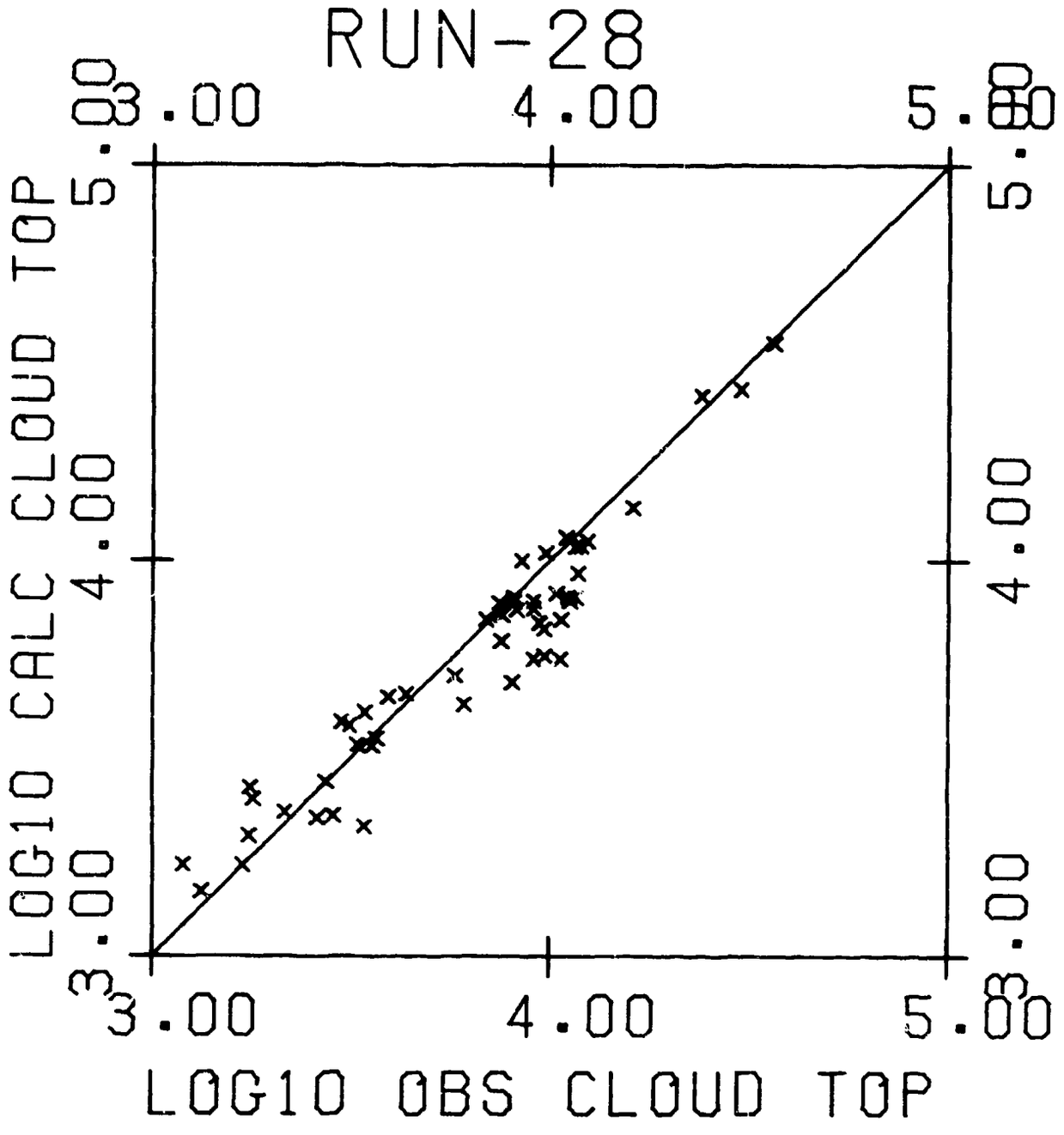

Figure 7a. Calculated vs. observed stabilized cloud top heights (meters relative to burst height) for 53 shots in the yield range 0.021-15,000 kT for the ref. 3 version of the CRM.

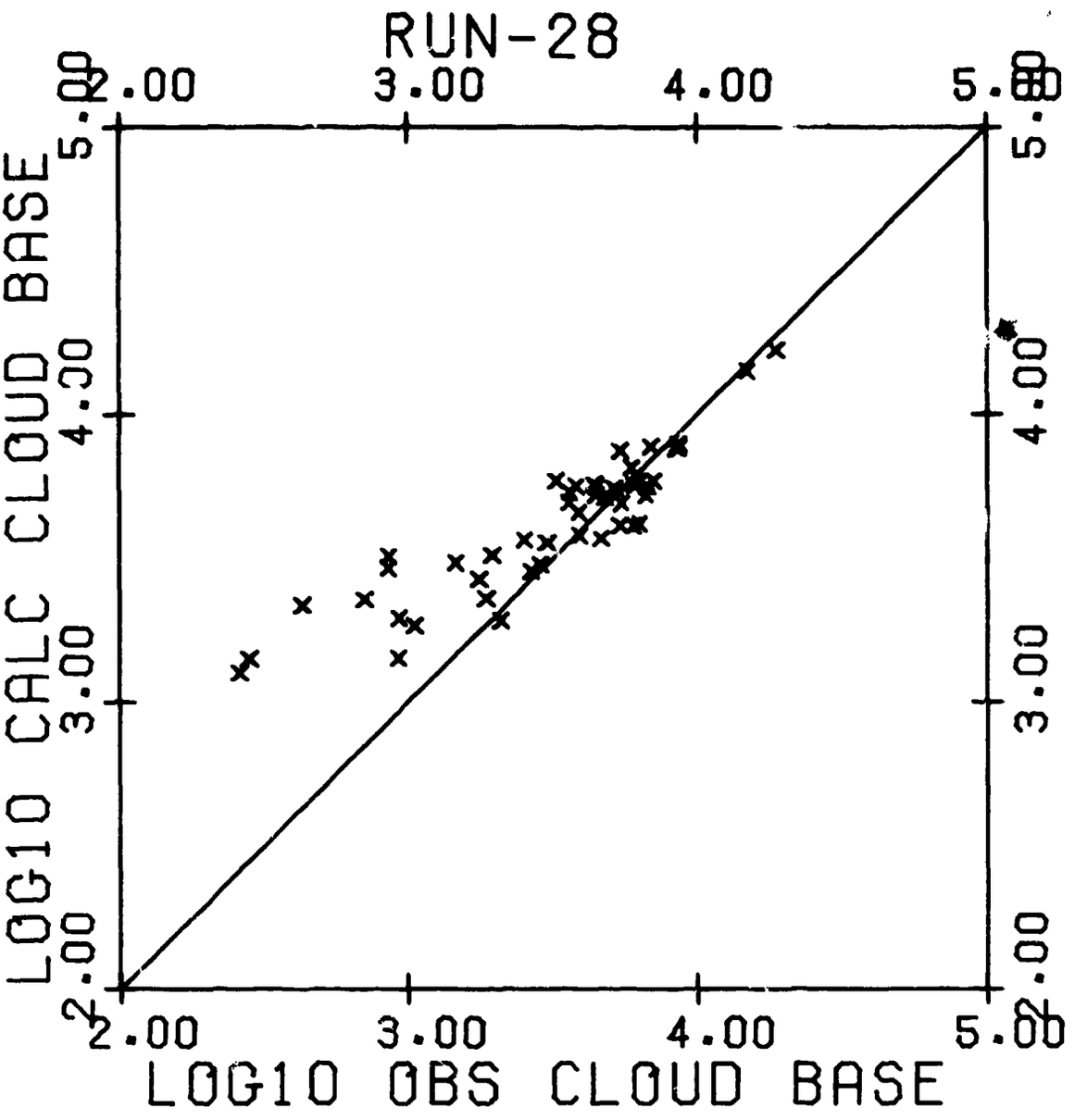

Figure 7b. Calculated vs. observed stabilized cloud base heights (meters relative to burst height) for 48 shots in the yield range 0.021-15,000 kT for the ref. 3 version of the CRM.

given by eq. (10) above. This change substantially reduces the initial rise velocity for low yield shots.

Figure 8 shows results for the CRM that are identical with the 1970 version except for this change in initial rise velocity. Comparison of Figs. 7 and 8 shows that reduction of the initial rise velocity results in an increased tendency to overpredict both tops and bases. This is a good illustration of the nonlinear character of the model. It also illustrates relatively high sensitivity of results for low yield shots to changes in initial rise velocity.

3.4.2 Sensitivity to k_2, μ, and f.

Prediction results are critically dependent on the values of the turbulence parameter, k_2, and the entrainment parameter, μ. Increase of k_2 causes increased conversion of rise energy to turbulent energy (eq. (4)), and increased turbulence drag on the cloud rise (eq. (1)): these effects combine to produce lower cloud heights. Increase in μ causes increased entrainment of air (eq. (5)), which in turn increases entrainment drag on the cloud rise (eq. (1)), reduces cloud temperature (eq. (3)), and dilutes turbulent energy density (eq. (4)). The overall effect is that lower cloud heights result from increased μ.

It should be understood that low yield shots are more sensitive to such changes than high yield shots. The reason is that high yield clouds are brought to rest in the stratosphere via action of the high stability encountered there, and thus their stabilized heights are primarily determined by the height of the tropopause and structure of the stratosphere.

In addition, it is important to know that effects of changes are not necessarily similar for shots of similar yields, and large changes in scatter can result from apparently minor adjustments of parameters.

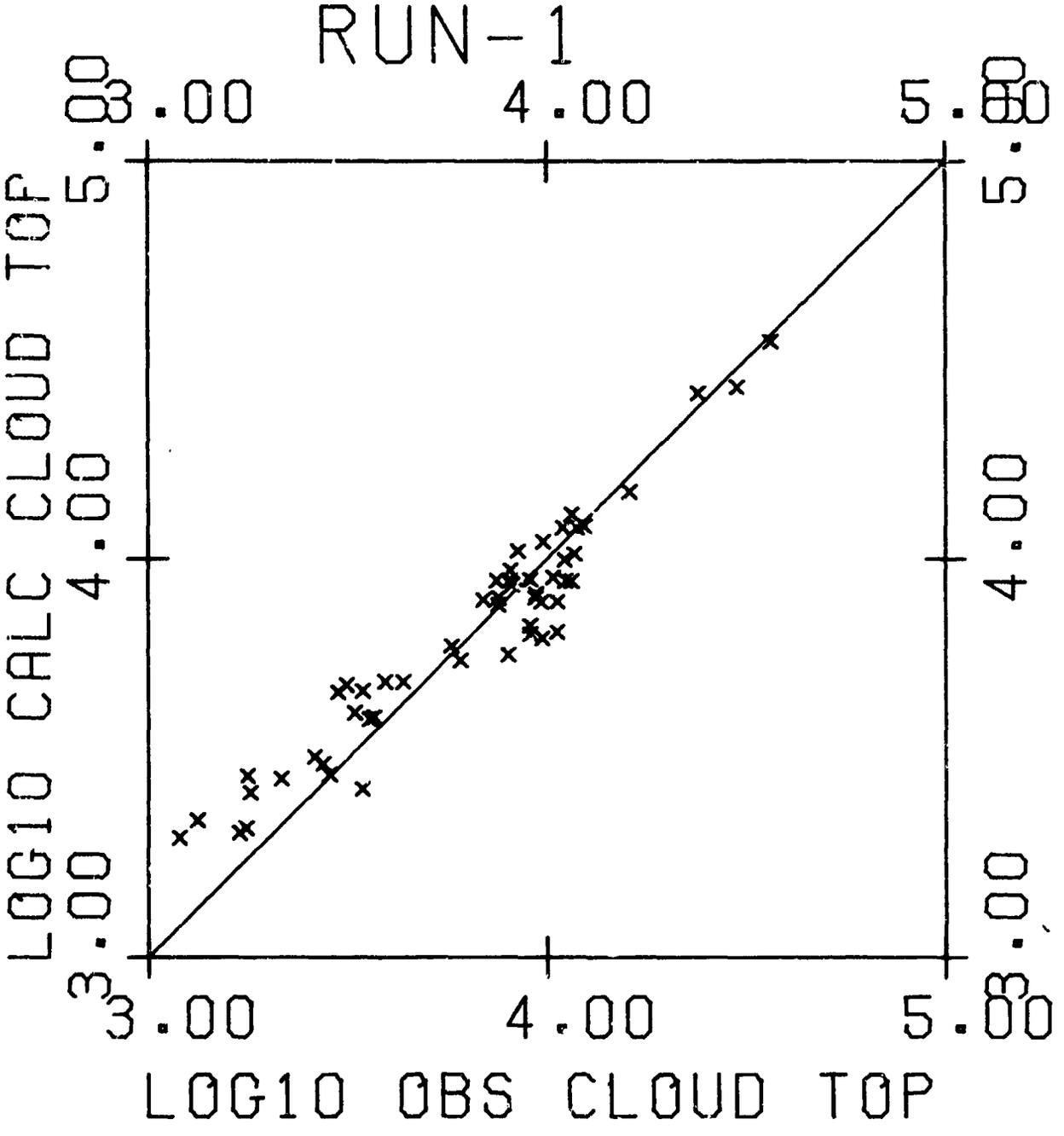

Figure 8a. Calculated vs. observed stabilized cloud top heights (meters relative to burst height) for 53 shots in the yield range 0.021-15,000 kT for the circa 1971 CRM.

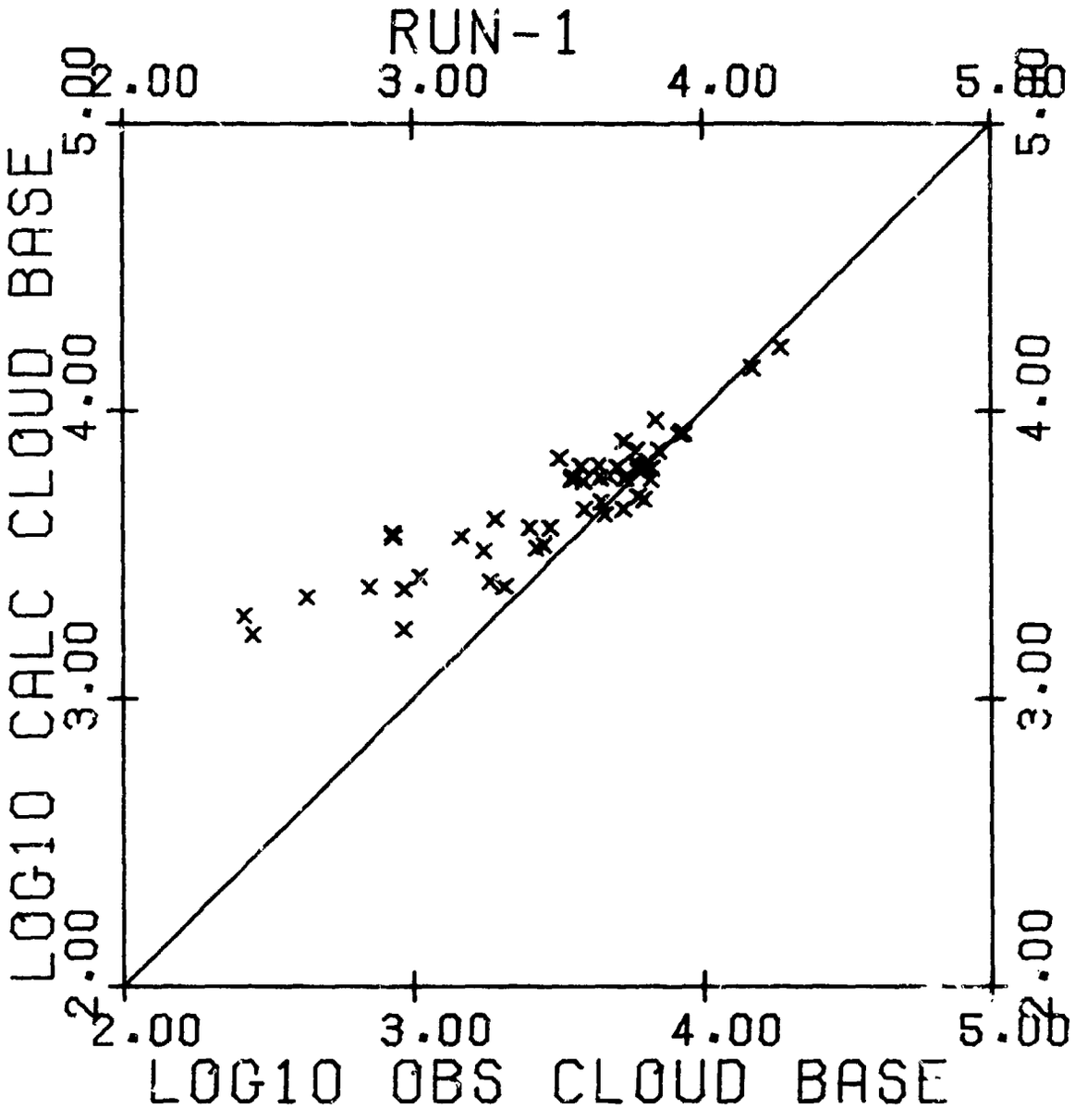

Figure 8b. Calculated vs. observed stabilized cloud base heights (meters relative to burst height) for 48 shots in the yield range 0.021-15,000 kT for the circa 1971 CRM.

As shown by eqs. (6) and (7), k_2 and μ are functions of yield over most of the yield range of interest. Extensive calculations, as illustrated by Fig. 9, have shown that it is not possible to adequately match calculated with observed results if single, yield independent values are used for these parameters.

For airbursts, stabilized cloud height is remarkably insensitive to change in explosion energy fraction, f, in the cloud. Variations in f from 20 to 50% produce only minor effects on cloud top and base heights. For surface bursts, on the other hand, large amounts of soil must be heated and the available energy must be sufficient for this. Thus, the interplay of initial soil temperature and f, discussed above on pp. 14,15 becomes important.

3.4.3 Sensitivity to Cloud Shape.

At each time step differential equations are integrated at the point of the cloud center, with atmospheric properties being taken for that point. Cloud volume is computed from mass of cloud air using the ideal gas law; therefore, the choice of cloud shape appears at first to be somewhat arbitrary.

Sensitivity studies show, however, that results are surprisingly sensitive to cloud shape. This is caused by the effects of changing the vertical radius, H_c, on the differential equations. H_c appears explicitly in eqs. (1) and (4), and in eq. (5) the factor S/V reduces to $3/H_c$ for an ellipsoidal cloud. Furthermore, shape interacts with parameters μ and k_2 in complex ways such that large variations in scatter are induced by minor variations in shape, apparently depending on the values of these other parameters.

Thus, one must proceed with caution in manipulating cloud shape since the consequences are much more than simply geometrical.

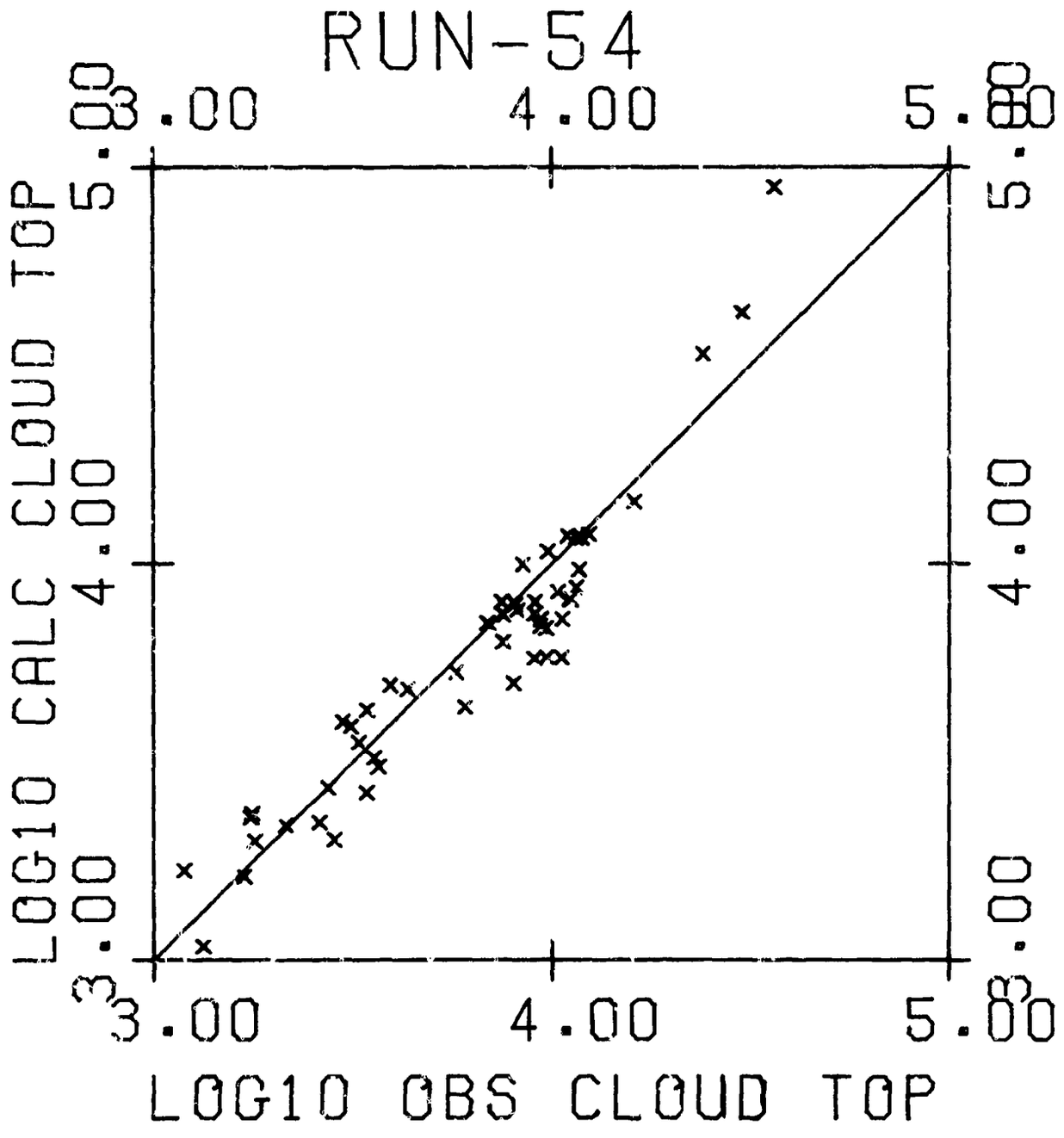

Figure 9a. Calculated vs. observed stabilized cloud top heights (meters relative to burst height) for 53 shots in the yield range 0.021-15,000 kT with constant k_2 and μ. The only substantial difference between this run and that of Fig. 2a is that k_2 and μ have values 0.1 and 0.12 for all yields.

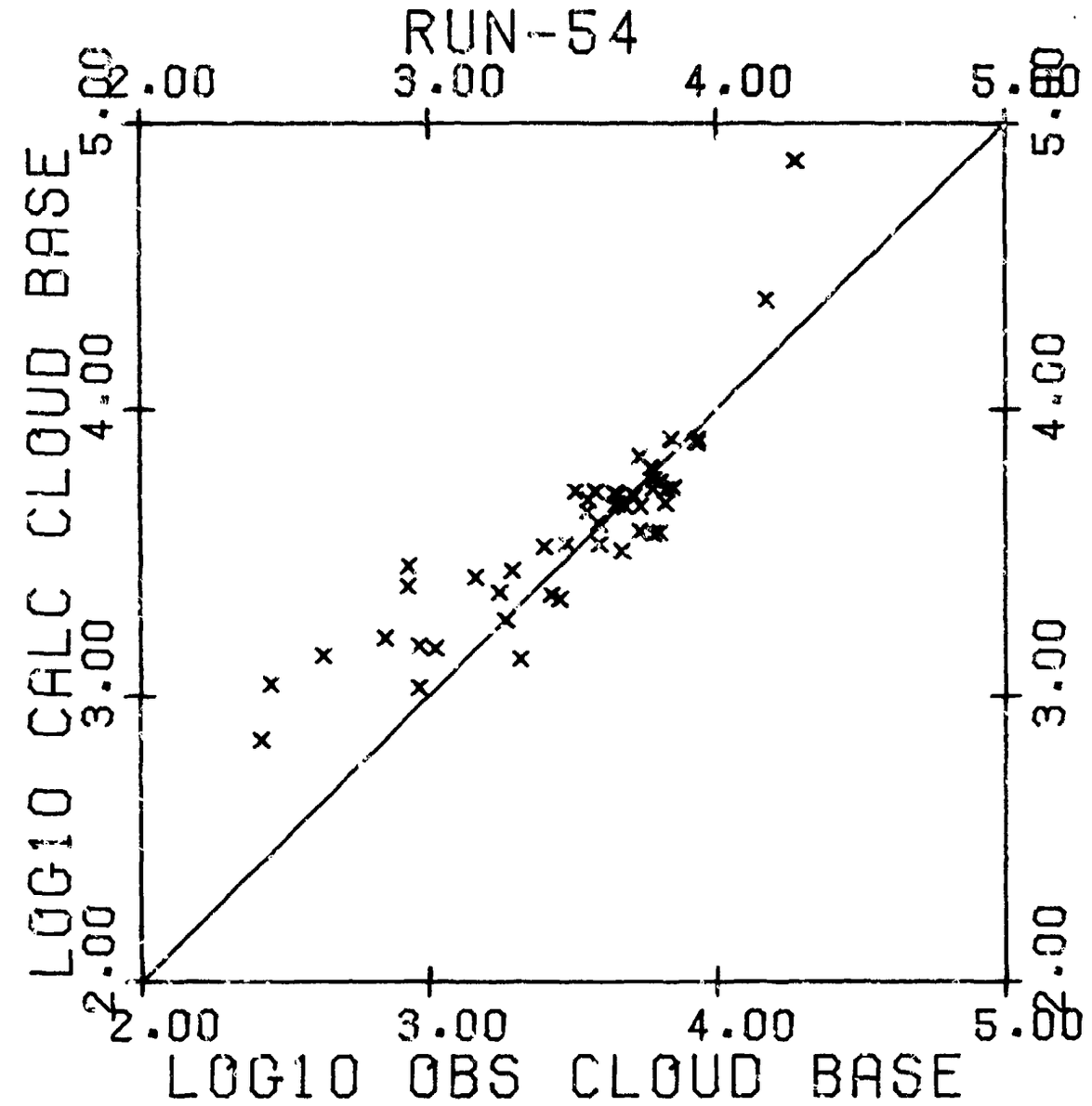

Figure 9b. Calculated vs. observed stabilized cloud base heights (meters relative to burst height) for 48 shots in the yield range 0.021-15,000 kT. The only substantial difference between this run and that of Fig. 2b is that k_2 and μ have values 0.1 and 0.12 for all yields.

4. EXTENSION TO VERY HIGH YIELDS

4.1 LIMITATIONS OF THEORY AND DATA

As already noted, the CRM differential equations are integrated at each time step at the point of the cloud center, using atmospheric conditions at the point. Cloud volume is computed from its air mass using the ideal gas law. Properties computed at the center are taken to be uniform throughout the cloud volume.

Even for low yield cases, the vertical span of a cloud is sufficient to cover a substantial range of atmospheric conditions. For large yield shots this span of conditions is immense. For example, at our initial time a 30 MT surface burst cloud with center at 2.8 km is computed to have a vertical diameter of 4.4km. At stabilization (using the 15°N annual standard atmosphere) its center is computed at 36 km with vertical diameter 26 km. For a 100 MT shot, initially the cloud center is computed at 4.2 km with vertical diameter 6.6 km, while at stabilization its center is at 39 km with vertical diameter 42 km.

The depth of the troposphere varies from roughly 10 - 15 km. Thus, at our initial time, the clouds may span from ¼ to more than ½ of the entire troposphere. The 100 MT stabilized cloud is computed to be distributed through the entire depth of the stratosphere, and even overlap into the mesosphere. Representation of such huge volumes by a point in the calculations stretches the credibility of the results.

On close examination of results for very high yield shots, one does indeed find non-physical behavior that is attributable to this model deficiency. For example, extremely low cloud temperatures ($T < 100°K$) are computed, and the cloud may actually lose mass for a short interval of time. This occurs because the factor S/V in eq. (5), which is proportional

to the ratio of cloud surface area to volume, necessarily becomes quite small for very large clouds. This results in decreased entrainment, which then increases velocity via reduced entrainment drag in eq. (1), which in turn acts via eq. (3) to increase temperature decay, etc. Obvious abnormal results are obtained and sometimes the calculation "crashes".

Of course, these problems occur to lesser extent for smaller clouds. However, for smaller yields ($W \leq 15$ MT) we can use observed data for calibration and validation. It is important to realize that the capability of the CRM depends as much on this validation as on the theoretical bases of the model. Consequently, in the yield range from 20 - 100 MT, prediction results should be considered as conjectural. The user must realize the theoretical shortcomings of the model when applied to very high yields, and he must realize that above 15 MT there has been no validation of results.

More satisfactory numerical simulations of large nuclear clouds would be provided by two- or three-dimensional, time-dependent hydrocodes, such as the SHELL code used by the Air Force Weapons Laboratory. However such codes have their own disadvantages, not least of which is that they require large amounts of computing time on even the most advanced computers. The one-dimensional code used in the CRM is ideal for fallout prediction needs, except as noted for extremely high yields.

4.2 ADJUSTMENT OF MODEL PARAMETERS

The yield dependent functions for k_2 and μ given by eqs. (6) and (7) were determined such as to produce best agreement between calculated and observed stabilized cloud top and base heights for the 53 observed cases described in sec. 3.1, which extend to 15 MT yield. When simulations first were attempted in

the yield range from 20 - 100 MT, I encountered a tendency for the cloud to "run away", and ultimately for the calculation to "crash". The main cause of this is as explained in the preceding section. In addition, the low values assigned k_2 for high yields decrease eddy-viscous drag in eq. (1), which compounds the problem. A straightforward remedy is to increase both k_2 and μ for very high yield cases. Thus, a lower limit of 0.004 was given to k_2, and above 19 MT the yield dependence of μ was changed from $W^{1/10}$ to $W^{1/3}$. These adjustments, which are expedient rather than empirical, enhance the probability that simulations will run to completion for yields up to 100 MT.*

---

* There can be no guarantee that "plausible" results will be obtained. For example, apparently minor defects in atmospheric data can cause trouble. Relative humidity data usually are not given at altitudes above 10 km in standard atmosphere tabulations. relative humidity is taken to be zero above 10 km, premature termination of cloud rise may occur in the yield range 50-100MT. This has been corrected by simply assuming reasonable values of relative humidity above 10 km.

REFERENCES

1. I.O. Huebsch, "The Development of a Water-Surface-Burst Fallout Model: The Rise and Expansion of the Atomic Cloud", USNRDL-TR-741 (23 April 1964). AD-441 983.

2. I.O. Huebsch, "Turbulence, Toroidal Circulation and Dispersion of Fallout Particles from the Rising Nuclear Cloud", USNRDL-TR-1054 (5 August 1966).

3. H.G. Norment and S. Woolf, "Department of Defense Land Fallout Prediction System. Vol. III - Cloud Rise (Revised)", DASA-1800-III (1 Sept. 1970). AD-879 890

4. H.G. Norment and S. Woolf, "Studies of Nuclear Cloud Rise and Growth", Technical Operations, Inc., unpublished.

5. H.G. Norment, W.Y.G. Ing and J. Zuckerman, "Department of Defense Land Fallout Prediction System. Vol. II - Initial Conditions", DASA-1800-II (30 Sept. 1966). AD-803 144

6. W.J. Klemm and J.C. Maloney, "Department of Defense Land Fallout Prediction System: Adaption for Extremely Low-Yield Detonations", BRL-MR-2452 (March 1975).

7. P.D. LaRiviere, et al., "Local Fallout from Nuclear Test Detonations. Vol. V. Transport and Distribution of Local (Early) Fallout from Nuclear Weapons Tests", SRI, unpublished.

8. J.E. Freund, Modern Elementary Statistics (Prentice-Hall, Inc. 1973). Sect. 11.2.

9. S. Glasstone, editor, The Effects of Nuclear Weapons (AEC, 1962).

10. H.G. Norment, "Cloud Rise Sensitivity of the Defense Land Fallout Interpretive Code (DELFIC)", ARCON Corp., unpublished.

11. I.O. Huebsch, "Analysis and Revision of the Cloud Rise Module of the Department of Defense Land Fallout Prediction System (DELFIC)", Euclid Research Group, BRL-CR-254 (May 1975). AD-B007 607L

APPENDIX A

GLOSSARY OF SYMBOLS
(mks units are used except where noted otherwise)

c_p	specific heat of air at constant pressure
d	differential operator
E	cloud turbulent kinetic energy density
f	fraction of the total explosion energy in the cloud at the initial time
g	gravity acceleration constant
H_c	vertical cloud radius
k_2	rise kinetic energy to turbulent energy conversion parameter (dimensionless)
k_3	turbulent energy dissipation constant (dimensionless)
m	cloud mass
m_i'	cloud virtual mass at the initial time
R_a	ideal gas law constant for air
R_c	horizontal cloud radius
S	$4\pi R_c^2$
t	time
T	cloud temperature (^oK)
T_e	ambient temperature
T_s	temperature of soil matter in the cloud

u	cloud center velocity
v	$\max(u, \sqrt{2E})$
V	cloud volume
W	explosion energy yield (kT)
z	vertical coordinate
ε	turbulent kinetic energy density dissipation rate in the cloud
μ	entrainment parameter (dimensionless)

APPENDIX B

REVIEW OF THE EUCLID RESEARCH GROUP ANALYSIS OF THE CLOUD RISE MODULE

B.1 INTRODUCTION

In an effort to remedy certain problems they were having with the DELFIC CRM, the Ballistics Research Laboratories retained Euclid Research Group (ERG) to analyse the CRM model described in ref. 3, and to recommend solutions to the problems. A report that contains the ERG analysis and recommendations has recently been published[11].

Those problems which in fact do exist are discussed and explained in the body of this report. The purpose of this review is to show the consequences of following the ERG recommendations, and to point out why these recommendations fail.

B.2 THE ERG ANALYSIS

The ERG analysis consists of three major parts:

- Consideration of the effects on energy transfer balance of two extraneous factors in the momentum equation (eq.(1)).
- An analysis of the entrainment equation (eq.(5)).
- Discussion of cloud shape.

Each of these is discussed below.

B.2.1. The Momentum Equation.

The momentum equation given in ref. 3 (eq.(1)) has two extraneous factors, $\frac{m}{m + m_i}$, which ERG labels the "virtual mass factor" (VMF), and $(1-\mu)$ which ERG inappropriately labels the "shape factor" (SF). The VMF factor is a relic of the original version of the CRM as developed by the Naval Radiological Defense Laboratory (NRDL). The SF factor was introduced by myself in the ref. 3 version of the CRM.

By means of a theoretical analysis, ERG shows that these factors cause imbalances in energy transfer in the cloud. Fortunately, it turns out that the factors have negligible effect on the cloud rise.* They have been deleted from the refined CRM.

B.2.2 The Entrainment Equation.

A key feature of the NRDL cloud rise model, developed by Huebsch[1], was the formulation of the entrainment equation. The success of the model was to considerable extent due to this formulation. In its original form, the equation was

$$\frac{dm}{dt} = \lambda \frac{S}{V} mv \quad , \tag{B.1}$$

where λ was a constant. Some years ago, I derived this form of the equation by combining the equation for mass conservation with

---

* See the last paragraphs in secs. 3.2.3. and 4.2.3. of the ERG report.

a simple function for vertical gradient of linear cloud dimension that was obtained from observed data. This analysis showed that additional terms are required in the entrainment equation (see Appendix C.1 of ref. 3), and the CRM model was revised accordingly.

ERG devotes considerable effort to rationalizations of why these changes in the entrainment equation cause problems with the simulations. The problems discussed in this connection are those that affect extremely high yield cloud simulations. These problems arise from the mathematical representation of the entire cloud volume by a point, a fundamental limitation of the model that is discussed in Chapter 4 above.

In fact the revised entrainment equation is theoretically sound. This is substantiated by the ERG energy transfer analysis, which shows total energy balance when the VMF and SF factors are removed. Furthermore, the form of the equation is solidly based on observed data. And finally, the appropriateness of the revised formulation is supported by the success of the model in simulating observed cloud behavior, as is well documented in the body of this report.

B.2.3 Cloud Shape.

As implied in sec. 2.5 above, the formulation of cloud shape in the context of this model has always been a minor problem. The formulation used in the ref. 3 version of the CRM is discussed in sec. 4.2.4 of the ERG report. I concur that that approach is less flexible than is desirable, and the possibility exists that unrealistic results may occur, though it does not happen in simulations of test shots. The new CRM uses an ellipsoidal cloud with eccentricity 0.75 as recommended by ERG. However this choice is not made for reasons of geometry alone, which is the sole basis of the ERG discussion.

It turns out (see sec. 3.4.3 above) that the overriding effect of manipulating cloud shape is to radically alter the rise via the effect of the vertical cloud radius, H_c, on the dynamics. Thus, the choice of an ellipsoidal cloud was made on the basis of comprehensive simulation results, and the particular eccentricity value was chosen to conform to observed cloud behavior[4].

B.3 THE ERG RECOMMENDATIONS

ERG makes the following recommendations for immediate implementation:

- Return the momentum and entrainment equations to the form used in the original NRDL version.
- Use an ellipsoidal cloud, eccentricity 0.75, until the cloud passes the tropopause or stops

rising, after which volume growth is accommodated by lateral expansion. (The NRDL version used this same algorithm except that a spherical, instead of ellipsoidal, cloud was used.)

- Set the parameters k_2 and μ to values of 0.1 and 0.25. (The NRDL version used values of 0.1 and 0.2 for these parameters.)

Implementation of these recommendations yields the results shown in Fig. B.1 — an obvious disaster. (See sec. 3.1 above for a description of the observed data set.) This may seem surprising since the model is so close to the one developed by Huebsch when he worked at NRDL. However, NRDL never performed a satisfactory validation study of their model, apparently being satisfied with results that were merely plausible.

B.4 CONCLUSIONS

The ERG recommendations amount to a return of the model substantially to its form of twelve years ago, as originally developed at the Naval Radiological Defense Laboratory for water surface bursts. As is shown by Fig. B.1, that version of the model is still unacceptable.

The ERG analysis is purely theoretical; no sensitivity computations were made to check conclusions arrived at by complicated rationalizations. Likewise, no attempt was made to determine the effects of recommended changes on model performance over the complete range of yields of interest. In light of the nonlinearity of results obtained by numerical solution of the twelve coupled differential equations that form the basis of the model, there is small wonder that the analysis failed in its objective.

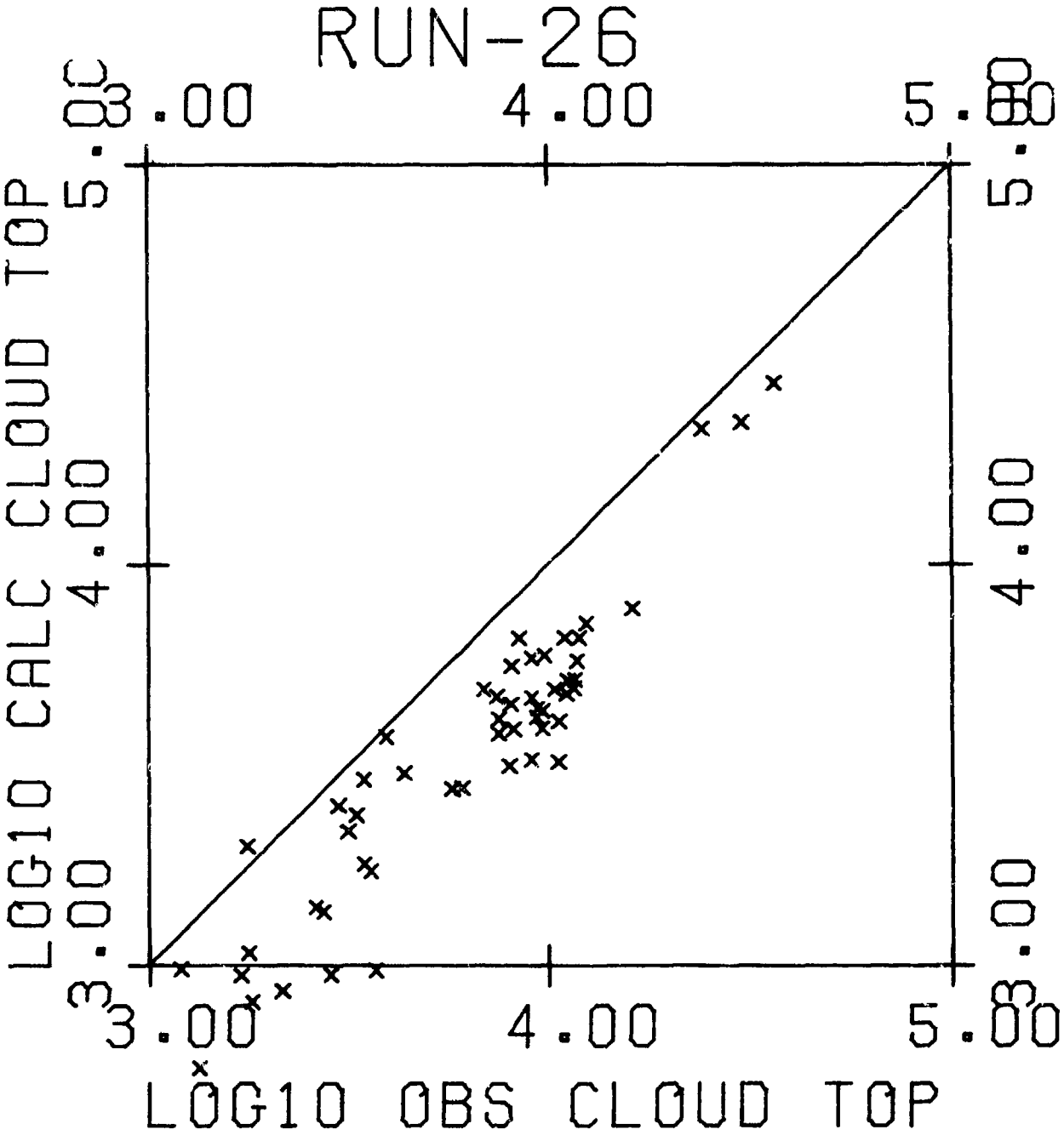

Figure B.1a. Calculated vs. observed stabilized cloud top heights (meters relative to burst height) for 53 shots in the yield range 0.021-15,000 kT for the CRM version recommended by Euclid Research Group.

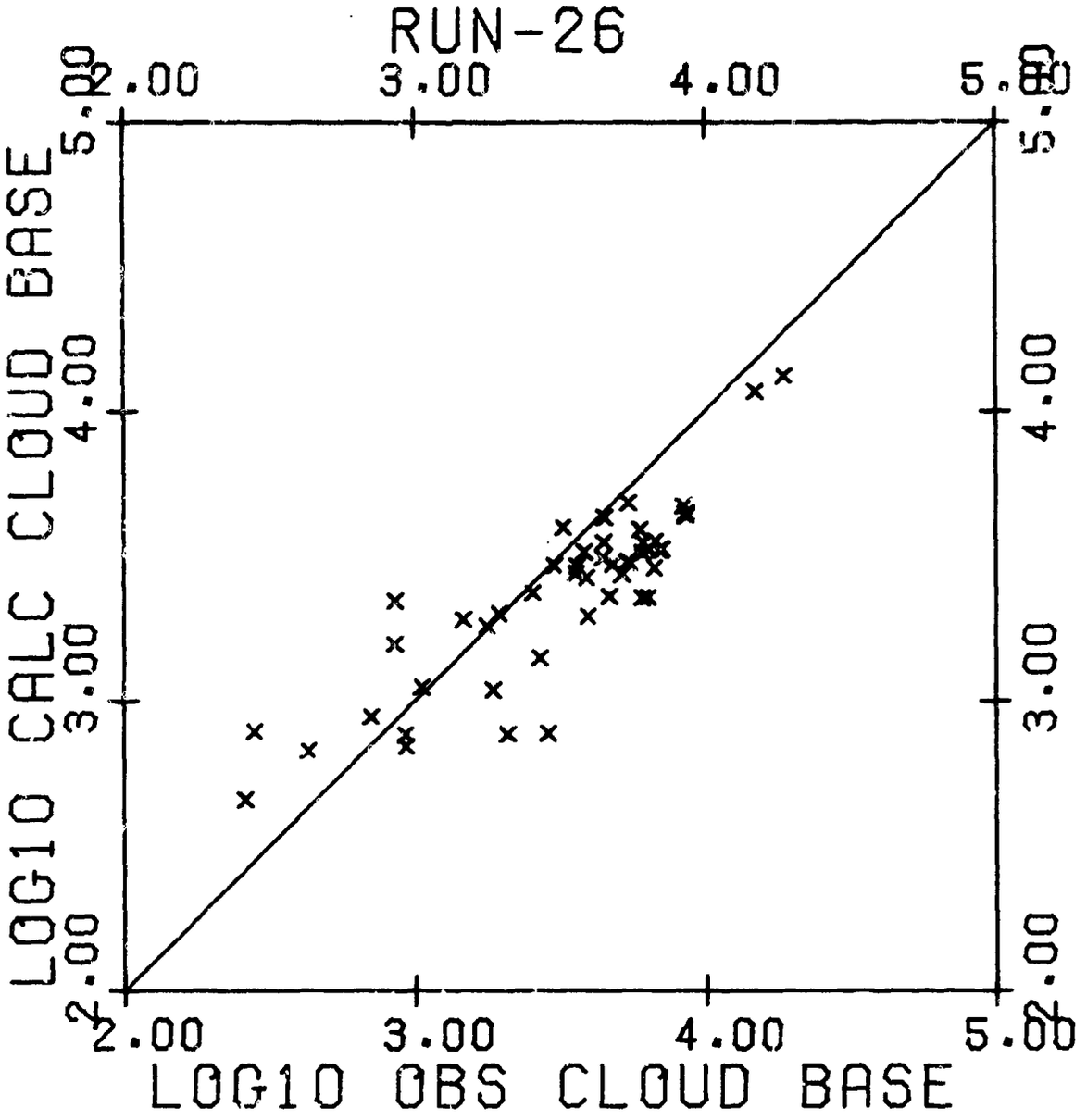

Figure B.2b. Calculated vs. observed stabilized cloud base heights (meters relative to burst height) for 48 shots in the yield range 0.021-15,000 kT for the CRM version recommended by Euclid Research Group.

DISTRIBUTION LIST

DEPARTMENT OF DEFENSE

Assistant Secretary of Defense
Program Analysis & Evaluation
Department of Defense
ATTN: Strat. Prgms.

Director
Defense Advanced Rsch. Proj. Agency
ATTN: Tech. Assessment Office
ATTN: NMRO
ATTN: Nuclear Monitoring Research
ATTN: Tactical Technology Office

Director
Defense Civil Preparedness Agency
Assistant Director for Research
ATTN: Postattack Research Division
ATTN: J. O. Buchanon

Defense Documentation Center
Cameron Station
12 cy ATTN: TC

Director
Defense Intelligence Agency
ATTN: DI-1
ATTN: DI-7
ATIN: DB-4C, Edward O'Farrell
ATTN: DI-7D, Major H. Ward

Director
Defense Nuclear Agency
ATTN: STRA
3 cy ATTN: TITL, Tech. Library
ATTN: TISI, Archives
ATTN: DDST
ATTN: RATN
ATTN: SPAS
ATTN: STSP
ATTN: STVL
ATTN: VLWS
ATTN: RAAE

Dir. of Defense Rsch. & Engineering
Department of Defense
ATTN: S&SS (OS)

Commander
Field Command
Defense Nuclear Agency
ATTN: FCPR, Major Kieltyka
ATTN: FCPR

Director
Interservice Nuclear Weapons School
ATTN: Doc. Con. for Major Talso

Chief
Livermore Division, Field Command, DNA
Lawrence Livermore Laboratory
ATTN: FCPRL

DEPARTMENT OF DEFENSE (Continued)

Chairman
Office of Joint Chiefs of Staff
ATTN: SAGA
ATTN: Technical Library

OJCS/J-3
ATTN: J-3

OJCS/J-5
ATTN: J-5

Director
Comd. Con. Tech. Center
ATTN: G. B. Adkins
ATTN: R. Mason
ATTN: G. Friend

DEPARTMENT OF THE ARMY

Dep. Chief of Staff for Rsch. Dev. & Acq.
Department of the Army
ATTN: NCB Division
ATTN: DAMA-CSM-N, LTC G. Ogden
ATTN: DAMA-CSM-N

Deputy Chief of Staff for Ops. & Plans
Department of the Army
ATTN: DAMO-SSN
ATTN: DAMO-ROS
ATTN: Tech. Advisor

Commander
Eighth US Army
ATTN: CJ-CO-A

Commander
Harry Diamond Laboratories
ATTN: DRXDO-TI, Tech. Lib.
ATTN: DRXDO-NP
ATTN: Chief Nuc. Vulnerability Branch

Commander
Picatinny Arsenal
ATTN: SARPA-ND-C, P. Angelotti

Director
TRASANA
ATTN: R. E. DeKinder, Jr.

Director
US Army Ballistic Research Labs.
2 cy ATTN: DRXBA-VL, J. Maloney

Commander
US Army Concepts Analysis Agency
ATTN: MOVA-WGP, Colonal Hincke

Commander
US Army Nuclear Agency
ATTN: ATCA-NAW
2 cy ATTN: Colonel R. Lounsbury

DEPARTMENT OF THE NAVY

Chief of Naval Research
Navy Department
ATTN: Code 464, Thomas P. Quinn

Commander
Naval Ocean Systems Center
ATTN: Tech. Lib. for T. J. Keary

Director
Naval Research Laboratory
ATTN: Code 2600, Tech. Lib.

Officer-in-Charge
Naval Surface Weapons Center
ATTN: Code WA501, Navy Nuc. Prgms. Off.

DEPARTMENT OF THE AIR FORCE

AF Weapons Laboratory, AFSC
ATTN: SAW
ATTN: DYT, Capt Daniel A. Matuska
ATTN: SUL

Headquarters
Air Force Systems Command
ATTN: DLSP, General Physics

Deputy Chief of Staff
Plans & Operations
Headquarters, US Air Force
ATTN: AFXOD

Hq. USAF/RD
ATTN: RLQSM

SAMSO/DY
ATTN: DYAE

ENERGY RESEARCH & DEVELOPMENT ADMINISTRATION

University of California
Lawrence Livermore Laboratory
ATTN: Thomas A. Gibson, L-125
ATTN: Joseph B. Knox, L-216
ATTN: Tech. Info. Dept. L-3
ATTN: George Staehle, L-24
ATTN: William J. Hogan, L-531
ATTN: M. Gustavson, L-21
ATTN: R. Barker, L-96
ATTN: T. Harvey

Los Alamos Scientific Laboratory
ATTN: Doc. Con. for L. Lowry
ATTN: Doc. Con. for W. Lyons
ATTN: Doc. Con. for R. Sandoval
ATTN: Doc. Con. for E. Chapin
ATTN: Doc. Con. for T. Dowler

Sandia Laboratories
ATTN: Doc. Con. for Org. 3422-1
ATTN: Doc. Con. for Sandia Rpt. Coll., Org. 3422-1
ATTN: Doc. Con. for M. L. Merritt
ATTN: Doc. Con. for Sandia Rpt. Coll., 3141

ENERGY RESEARCH & DEVELOPMENT ADMINISTRATION (Continued)

US Energy Rsch. & Dev. Admin.
Division of Headquarters Services
Library Branch G-043
ATTN: Doc. Con. for Class Tech. Lib.
ATTN: Doc. Con. for H. C. Hollister

DEPARTMENT OF DEFENSE CONTRACTORS

Atmospheric Science Associates
ATTN: Hillyer G. Norment

The BDM Corporation
ATTN: Joseph V. Braddock

General Electric Company
TEMPO-Center for Advanced Studies
ATTN: DASIAC

Mathematical Applications Group, Inc. (NY)
ATTN: Martin O. Cohen

McMillan Science Associates, Inc.
ATTN: Robert Oliver

Mission Research Corporation
ATTN: Dave Sowle

Pacific-Sierra Research Corp.
ATTN: Gary Lang

Physics International Company
ATTN: Doc. Con. for Michael McKay

R & D Associates
ATTN: C. MacDonald
ATTN: Richard Montgomery
ATTN: Harold L. Brode

The Rand Corporation
ATTN: R. Robert Rapp
ATTN: Technical Library

Stanford Research Institute
ATTN: Stephen L. Brown
ATTN: Philip J. Dolan
ATTN: R. Rodden

Science Applications
ATTN: J. McGohan